Spin axis evolution of two interacting bodies

G. Boué, J. Laskar

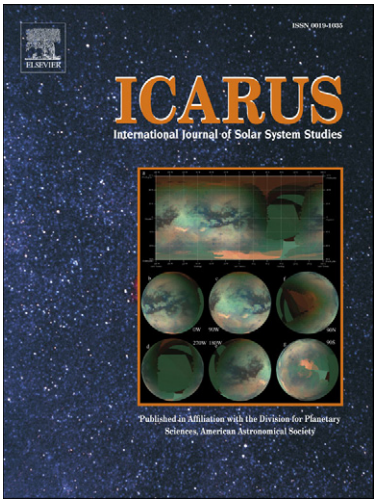

Spin axis evolution of two interacting bodies

G. Boué, J. Laskar

PII: S0019-1035(09)00038-4
DOI: 10.1016/j.icarus.2009.02.001
Reference: YICAR 8898

To appear in: *Icarus*

Received date: 12 December 2008
Revised date: 3 February 2009
Accepted date: 4 February 2009

Please cite this article as: G. Boué, J. Laskar, Spin axis evolution of two interacting bodies, *Icarus* (2009), doi: 10.1016/j.icarus.2009.02.001

Spin axis evolution of two interacting bodies.

G. Boué and J. Laskar

Astronomie et Systèmes Dynamiques, IMCCE-CNRS UMR8028,

Observatoire de Paris, 77 Av. Denfert-Rochereau, 75014 Paris, France

February 3, 2009

PAGES: 66 ; TABLES: 8 ; FIGURES: 8

Running Title : Spin axis evolution of two interacting bodies.

Corresponding author : Gwenaël Boué

Astronomie et Systèmes Dynamiques, IMCCE-CNRS UMR8028,

Observatoire de Paris, 77 Av. Denfert-Rochereau, 75014 Paris, France

email : boue@imcce.fr

Abstract

We consider the solid-solid interactions in the two body problem. The relative equilibria have been previously studied analytically and general motions were numerically analyzed using some expansion of the gravitational potential up to the second order, but only when there are no direct interactions between the orientation of the bodies. Here we expand the potential up to the fourth order and we show that the secular problem obtained after averaging over fast angles, as for the precession model of Boué and Laskar [Boué, G., Laskar, J., 2006. Icarus 185, 312–330] , is integrable, but not trivially. We describe the general features of the motions and we provide explicit analytical approximations for the solutions. We demonstrate that the general solution of the secular system can be decomposed as a uniform precession around the total angular momentum and a periodic symmetric orbit in the precessing frame. More generally, we show that for a general n-body system of rigid bodies in gravitational interaction, the regular quasiperiodic solutions can be decomposed into a uniform precession around the total angular momentum, and a quasiperiodic motion with one frequency less in the precessing frame.

Keywords : CELESTIAL MECHANICS, SOLID-SOLID INTERACTION, BINARY ASTEROID DYNAMICS, ROTATIONAL DYNAMICS

1 Introduction

We consider here two rigid bodies orbiting each other. The main purpose of this work is to determine the long term evolution of their spin orientation and to a lower extent, the orientation of the orbital plane. Examples of such systems are binary asteroids or a planet with a massive satellite.

If the two bodies are spherical, then the translational and the rotational motions are independent (e.g. Duboshin, 1958). In that case, the orbit is purely keplerian and the proper rotation of the bodies are uniform. General problems with triaxial bodies are more complicated, and usually non integrable. Even formal expansions of the gravitational potential or the proof of their convergence can be an issue (Borderies, 1978; Paul, 1988; Tricarico, 2008). In some cases, especially for slow rotations close to low order spin-orbit resonances, the spin evolution of rigid bodies of irregular shape can be strongly chaotic (Wisdom et al., 1984; Wisdom, 1987), but we will not consider this situation in the present paper where we focus on regular and quasiperiodic motions.

Stationary solutions of spin evolution are known in the case of a triaxial satellite orbiting a central spherical planet (Abul'naga and Barkin, 1979). In their paper, Abul'naga and Barkin used canonical coordinates, based on the Euler angles, to set the orientation of the satellite. On the contrary, in 1991, Wang et al. also studied relative equilibria but with a vectorial approach that enabled them to analyze easily the stability of those solutions. For a review of different formalisms that can be used in rigid body problems, see (Borisov and Mamaev, 2005).

The vectorial approach turned out to be also powerful for the study of relative equilibria of two triaxial bodies orbiting each other (Maciejewski, 1995). General motions of this problem were studied by Fahnestock and Scheeres in 2008 (hereafter FS08) in the case of the typical binary asteroid system called 1999 KW4. For that, the authors expanded the gravitational potential up to the second order only. In this approximation, there is no direct interaction between the orientation of the two bodies. Ashenberg gave in 2007 the expression of the gravitational potential expanded up to the fourth order but didn't study the solutions.

In (Boué and Laskar, 2006) (hereafter BL06) we gave a new method to study the long term evolution of solid body orientations in the case of a star-planet-satellite problem where only the planet is assumed to be rigid. This method used a similar vectorial approach as Wang et al. (1991), plus some averaging over the fast angles. We showed that the secular evolution of this system is integrable and provided the general solution.

In the present paper, we show that the problem of two triaxial bodies orbiting each other is very similar to the star-planet-satellite problem and thus can be treated in the same way.

In the section 2, we compute the Hamiltonian governing the evolution of two interacting rigid bodies. The gravitational potential is expanded up to the fourth order and averaged over fast angles. The resulting secular Hamiltonian is a function of three vectors only: the orbital angular momentum and the angular momenta of the two bodies.

In a next step (section 3), we show that the secular problem is integrable but not trivially (i.e. it cannot be reduced to a scalar first order differential equation that can be integrated by quadrature). The general solution is the product of a uniform rotation of the three vectors (global precession around the total angular momentum) by a periodic motion (nutation). We prove also that in a frame rotating with the precession frequency, the nutation loops described by the three vectors are all symmetric with respect to a same plane containing the total angular momentum. We then derive analytical approximations of the two frequencies of the secular problem with their amplitudes. These formulas need averaged quantities that can be computed recursively. However we found that the first iteration already gives satisfactory results.

In section 5, we consider the general case of a n-body system of rigid bodies in gravitational interaction, and we demonstrate that the regular quasiperiodic solutions of these systems can, in a similar way, be decomposed into a uniform precession, and a quasiperiodic motion in the precessing frame.

Finally, we compare our results with those of FS08 on the typical binary asteroid system 1999 KW4. We show that their analytical expression of the precession frequency corresponds to the simple case of a point mass orbiting an oblate body treated in BL06. We then integrate numerically from the full Hamiltonian, an example of a doubly asynchronous system where the

FS08 expression of the precession frequency does not apply. We compare the results with the output of the averaged Hamiltonian and with our numerical approximation and show that they are in good agreement.

2 Fundamental equations

We are considering a two rigid body problem in which the interaction is purely gravitational with no dissipative effects. Let m_1 and m_2 be the masses of the two solids. Hereafter the mass m_2 is called the satellite or the secondary and the mass m_1 the primary. It should be stressed that this notation does not imply any constraint on the ratio of the masses which can even be equal to one.

The configuration of the system is described by the position vector $\mathbf{r}$ of the satellite barycenter relative to the primary barycenter and their orientation expressed in an invariant reference frame. The orientations are given by the coordinates of the principal axes $(\boldsymbol{I}_1, \boldsymbol{J}_1, \boldsymbol{K}_1)$ and $(\boldsymbol{I}_2, \boldsymbol{J}_2, \boldsymbol{K}_2)$ in which the two inertia tensors, respectively $\mathcal{I}_1$ and $\mathcal{I}_2$, of the primary and of the secondary are diagonal [$\mathcal{I}_1 = \mathrm{diag}(A_1, B_1, C_1)$ and $\mathcal{I}_2 = \mathrm{diag}(A_2, B_2, C_2)$].

The Hamiltonian of this problem can be split into

$$\mathcal{H} = H_T + H_E + H_I \tag{1}$$

where H_T is the Hamiltonian of the free translation of the reduced point mass $\beta = m_1 m_2/(m_1 + m_2)$, H_E describes the free rigid rotation of the two bodies and H_I contains the gravitational interaction.

The Hamiltonian of the free point mass is

$$H_T = \frac{\tilde{\mathbf{r}}^2}{2\beta} \tag{2}$$

where $\tilde{\mathbf{r}} = \beta\dot{\mathbf{r}}$ is the conjugate momentum of $\mathbf{r}$.

Let $\boldsymbol{G}_1$ and $\boldsymbol{G}_2$ be respectively the angular momentum of the primary and of the satellite. The Hamiltonian of the free rotation is

$$H_E = \frac{{}^t\boldsymbol{G}_1 \mathcal{I}_1^{-1} \boldsymbol{G}_1}{2} + \frac{{}^t\boldsymbol{G}_2 \mathcal{I}_2^{-1} \boldsymbol{G}_2}{2}, \tag{3}$$

where the superscript ^{t} in ${}^t\mathbf{x}$ or ${}^tA$ denotes the transpose of any vector $\mathbf{x}$ or matrix A. It can be expressed in terms of the principal bases of the two bodies as follows

$$H_E = \frac{(\boldsymbol{G}_1\cdot \boldsymbol{I}_1)^2}{2A_1} + \frac{(\boldsymbol{G}_1\cdot \boldsymbol{J}_1)^2}{2B_1} + \frac{(\boldsymbol{G}_1\cdot \boldsymbol{K}_1)^2}{2C_1} + \frac{(\boldsymbol{G}_2\cdot \boldsymbol{I}_2)^2}{2A_2} + \frac{(\boldsymbol{G}_2\cdot \boldsymbol{J}_2)^2}{2B_2} + \frac{(\boldsymbol{G}_2\cdot \boldsymbol{K}_2)^2}{2C_2}. \quad (4)$$

The interaction between the two solid bodies is the following double integral

$$H_I = -\iint \frac{\mathcal{G}\, dm_1\, dm_2}{\|\mathbf{r}+\mathbf{r}_2-\mathbf{r}_1\|} \quad (5)$$

where $\mathbf{r}_1$ and $\mathbf{r}_2$ are respectively computed relative to the primary and satellite barycenters (cf Fig. 1) and describe the two volumes. This part of the Hamiltonian can be expanded in terms of Legendre polynomials and will be written as a function of $(\mathbf{r}, \boldsymbol{I}_1, \boldsymbol{J}_1, \boldsymbol{K}_1, \boldsymbol{I}_2, \boldsymbol{J}_2, \boldsymbol{K}_2)$ in the section 2.3.

2.1 Equations of motion

The full Hamiltonian is written in the non-canonical coordinates $(\mathbf{r}, \tilde{\mathbf{r}}, \boldsymbol{I}_1, \boldsymbol{J}_1, \boldsymbol{K}_1, \boldsymbol{G}_1, \boldsymbol{I}_2, \boldsymbol{J}_2, \boldsymbol{K}_2, \boldsymbol{G}_2)$. Thus, although the components $(\mathbf{r}, \tilde{\mathbf{r}})$ keep the standard symplectic structure, $(\boldsymbol{I}_1, \boldsymbol{J}_1, \boldsymbol{K}_1, \boldsymbol{G}_1)$ on the one hand and $(\boldsymbol{I}_2, \boldsymbol{J}_2, \boldsymbol{K}_2, \boldsymbol{G}_2)$ on the other hand possess the Euler-Poisson structure which leads to the following equations of motion (Borisov and Mamaev, 2005)

$$\begin{aligned} &\dot{\mathbf{r}} = \boldsymbol{\nabla}_{\tilde{\mathbf{r}}}\mathcal{H}, \quad \dot{\tilde{\mathbf{r}}} = -\boldsymbol{\nabla}_{\mathbf{r}}\mathcal{H} \\ &\dot{\boldsymbol{G}} = \boldsymbol{\nabla}_{\boldsymbol{I}}\mathcal{H}\times\boldsymbol{I} + \boldsymbol{\nabla}_{\boldsymbol{J}}\mathcal{H}\times\boldsymbol{J} + \boldsymbol{\nabla}_{\boldsymbol{K}}\mathcal{H}\times\boldsymbol{K} + \boldsymbol{\nabla}_{\boldsymbol{G}}\mathcal{H}\times\boldsymbol{G} \\ &\dot{\boldsymbol{I}} = \boldsymbol{\nabla}_{\boldsymbol{G}}\mathcal{H}\times\boldsymbol{I}, \quad \dot{\boldsymbol{J}} = \boldsymbol{\nabla}_{\boldsymbol{G}}\mathcal{H}\times\boldsymbol{J}, \quad \dot{\boldsymbol{K}} = \boldsymbol{\nabla}_{\boldsymbol{G}}\mathcal{H}\times\boldsymbol{K}. \end{aligned} \quad (6)$$

We choose these non-canonical coordinates instead of symplectic ones because of the simplicity of the resulting equations which already resemble equations of precession.

2.2 First simplification

In the previous paragraphs, the Hamiltonian contains the three vectors of the principal frame $(\boldsymbol{I}, \boldsymbol{J}, \boldsymbol{K})$ of each body. Nevertheless, only two vectors per solid are necessary insofar as the third can be expressed as the wedge product of the other two. We choose to keep $\boldsymbol{I}$ and $\boldsymbol{K}$.

The Hamiltonian of the free rotation of the two rigid bodies can be rewritten as follows

$$\begin{aligned} H_E = \frac{\boldsymbol{G}_1^2}{2B_1} + \frac{\boldsymbol{G}_2^2}{2B_2} \\ + \left(\frac{1}{A_1} - \frac{1}{B_1}\right)\frac{(\boldsymbol{G}_1 \cdot \boldsymbol{I}_1)^2}{2} + \left(\frac{1}{C_1} - \frac{1}{B_1}\right)\frac{(\boldsymbol{G}_1 \cdot \boldsymbol{K}_1)^2}{2} \\ + \left(\frac{1}{A_2} - \frac{1}{B_2}\right)\frac{(\boldsymbol{G}_2 \cdot \boldsymbol{I}_2)^2}{2} + \left(\frac{1}{C_2} - \frac{1}{B_2}\right)\frac{(\boldsymbol{G}_2 \cdot \boldsymbol{K}_2)^2}{2}. \end{aligned} \quad (7)$$

2.3 Gravitational potential

The distance between the two bodies is assumed to be large in comparison to their size. Thus, in the expression of the gravitational potential (5), $\rho_1 = \|\mathbf{r}_1\| / \|\mathbf{r}\|$ and $\rho_2 = \|\mathbf{r}_2\| / \|\mathbf{r}\|$ are two small parameters. It can then be expanded in terms of Legendre polynomials (see Appendix A). As it is shown below (equation 13), the expansion up to the second order does not contain any interaction due to the relative orientation of the bodies. We thus choose to expand the gravitational potential up to the fourth order. In the computation appear integrals such as $\int r_i^2 \, dm_i$ or $\int {\mathbf{r}_i}^t \mathbf{r}_i \, dm_i$, $i = 1, 2$ which can be expressed in terms of moments of inertia

$$\begin{aligned} \int r_i^2 \, dm_i &= \frac{A_i + B_i + C_i}{2} \; ; \\ \int {\mathbf{r}_i}^t \mathbf{r}_i \, dm_i &= \frac{A_i - B_i + C_i}{2} Id + (B_i - A_i) {\boldsymbol{I}_i}^t \boldsymbol{I}_i + (B_i - C_i) {\boldsymbol{K}_i}^t \boldsymbol{K}_i \; , \end{aligned} \quad (8)$$

with Id beeing the identity matrix in $\mathbb{R}^3$. But higher degree integrals such as $\int r_i^4 \, dm_i$ also appear. To compute these integrals, one needs more information about the bodies. However, moments of inertia are already hardly known, at least for satellites. It is thus not relevant to add new unconstrained parameters. But such integrals of inertia can be expressed as functions of A_i, B_i, C_i assuming that the bodies are homogeneous ellipsoids. Indeed, let (x_i, y_i, z_i) be the coordinates in the principal frame of a running point of the body i, and $I_{p,q,r;i} = \int x_i^p y_i^q z_i^r \, dm_i$ be

its integrals of inertia. Because of the three symmetry planes of homogeneous ellipsoids, $I_{p,q,r;i}$ vanishes whenever one of p, q, r is odd. Thus all the third order integrals of inertia cancel, and the only non zero fourth order integrals of inertia are (see Appendix B)

$$\begin{aligned}
\int x_i^4\, dm_i &= \frac{15}{28m_i}(-A_i+B_i+C_i)^2 \ ; \\
\int y_i^4\, dm_i &= \frac{15}{28m_i}(A_i-B_i+C_i)^2 \ ; \\
\int z_i^4\, dm_i &= \frac{15}{28m_i}(A_i+B_i-C_i)^2 \ ; \\
\int y_i^2 z_i^2\, dm_i &= \frac{5}{28m_i}(A_i-B_i+C_i)(A_i+B_i-C_i) \ ; \\
\int z_i^2 x_i^2\, dm_i &= \frac{5}{28m_i}(A_i+B_i-C_i)(-A_i+B_i+C_i) \ ; \\
\int x_i^2 y_i^2\, dm_i &= \frac{5}{28m_i}(-A_i+B_i+C_i)(A_i-B_i+C_i) \ .
\end{aligned} \tag{9}$$

In search of generality, we now forget the assumption of homogeneous ellipsoids. We only keep the symmetry plane hypothesis that cancels odd integrals. Setting

$$\begin{aligned}
X_i &= \int x_i^4\, dm_i \qquad P_i = \int y_i^2 z_i^2\, dm_i \ ; \\
Y_i &= \int y_i^4\, dm_i \qquad Q_i = \int z_i^2 x_i^2\, dm_i \ ; \\
Z_i &= \int z_i^4\, dm_i \qquad R_i = \int x_i^2 y_i^2\, dm_i
\end{aligned} \tag{10}$$

the integrals appearing in the expansion of the gravitational potential become

$$\begin{aligned}
\int r_i^4\, dm_i &= X_i + Y_i + Z_i + 2P_i + 2Q_i + 2R_i \ ; \\
\int (\boldsymbol{s}\cdot \mathbf{r}_i)^4\, dm_i &= Y_i \boldsymbol{s}^4 + (X_i + Y_i - 6R_i)(\boldsymbol{s}\cdot \boldsymbol{I}_i)^4 \\
&\quad +(Z_i + Y_i - 6P_i)(\boldsymbol{s}\cdot \boldsymbol{K}_i)^4 \\
&\quad +2\boldsymbol{s}^2[(3R_i - Y_i)(\boldsymbol{s}\cdot \boldsymbol{I}_i)^2 + (3P_i - Y_i)(\boldsymbol{s}\cdot \boldsymbol{K}_i)^2] \\
&\quad +2[Y_i - 3(P_i - Q_i + R_i)](\boldsymbol{s}\cdot \boldsymbol{I}_i)^2(\boldsymbol{s}\cdot \boldsymbol{K}_i)^2 \ ; \\
\int r_i^2 \mathbf{r}_i{}^t \mathbf{r}_i\, dm_i &= (Y_i + R_i + P_i) Id + (X_i - Y_i + Q_i - P_i)\boldsymbol{I}_i{}^t \boldsymbol{I}_i \\
&\quad +(Z_i - Y_i + Q_i - R_i)\boldsymbol{K}_i{}^t \boldsymbol{K}_i
\end{aligned} \tag{11}$$

where $\boldsymbol{s}$ is any vector and $i = 1, 2$.

With these results, the expansion of the potential gives the zeroth order term

$$H_I^{(0)} = -\frac{\mu\beta}{r} \tag{12}$$

where $\mu = \mathcal{G}(m_1 + m_2)$. This is the well known gravitational interaction between two point masses. The second order terms expression is classical and given by

$$H_I^{(2)} = -\frac{1}{2}\frac{\mathcal{G}}{r^3}\left[m_1(A_2 - 2B_2 + C_2) + m_2(A_1 - 2B_1 + C_1)\right] - \frac{3}{2}\frac{\mathcal{G}m_1}{r^3}\left[(B_2 - A_2)\,(\mathbf{u}\cdot\boldsymbol{I}_2)^2 + (B_2 - C_2)\,(\mathbf{u}\cdot\boldsymbol{K}_2)^2\right] - \frac{3}{2}\frac{\mathcal{G}m_2}{r^3}\left[(B_1 - A_1)\,(\mathbf{u}\cdot\boldsymbol{I}_1)^2 + (B_1 - C_1)\,(\mathbf{u}\cdot\boldsymbol{K}_1)^2\right] \quad (13)$$

where $\mathbf{u} = \mathbf{r}/r$ is the direction vector of r. As mentioned before, this expression does not contain body-body interactions but only spin-orbit ones such as $(\mathbf{u}\cdot\boldsymbol{K}_1)^2$ or $(\mathbf{u}\cdot\boldsymbol{K}_2)^2$. The fourth order terms expression is given in (14). In contrast to the second order terms, among the fourth order terms there are direct interactions between the two orientations such as $(\boldsymbol{K}_1\cdot\boldsymbol{K}_2)^2$. A similar expression was published recently in (Ashenberg, 2007). Although more terms are present in Ashenberg's paper because we have made here the additional assumption of symmetry of the rigid bodies, we could compare our expression successfully with the one of Ashenberg, except for a difference in a coefficient that may come from a misprint in Ashenberg's paper[1].

[1]In (Ashenberg, 2007), there is a misprint in the expression of $V^{(4)}_{BB'}$, Eq. (20). The coefficient $-3\mathcal{G}/(4r^5)$ in Eq. (14) of the current paper corresponds to a coefficient $-G/(8R^5)$ in Ashenberg's notations whereas it is written $-G/(5R^5)$ in (Ashenberg, 2007).

$$
\begin{aligned}
H_I^{(4)} = -\frac{3}{4}\frac{\mathcal{G}}{r^5}\Bigg\{ & (A_2 - 2B_2 + C_2)(A_1 - 2B_1 + C_1) \\
& + \frac{1}{2}m_2[X_1 + \frac{8}{3}Y_1 + Z_1 - 8P_1 + 2Q_1 - 8R_1] \\
& + \frac{1}{2}m_1[X_2 + \frac{8}{3}Y_2 + Z_2 - 8P_2 + 2Q_2 - 8R_2] \\
& + 2(B_1 - A_1)(B_2 - A_2)(\boldsymbol{I}_1 \cdot \boldsymbol{I}_2)^2 \\
& + 2(B_1 - A_1)(B_2 - C_2)(\boldsymbol{I}_1 \cdot \boldsymbol{K}_2)^2 \\
& + 2(B_1 - C_1)(B_2 - A_2)(\boldsymbol{K}_1 \cdot \boldsymbol{I}_2)^2 \\
& + 2(B_1 - C_1)(B_2 - C_2)(\boldsymbol{K}_1 \cdot \boldsymbol{K}_2)^2 \\
& + \Big[5(A_2 - 2B_2 + C_2)(B_1 - A_1) \\
& \qquad - m_2(5X_1 + \frac{20}{3}Y_1 - 5P_1 + 5Q_1 - 35R_1)\Big](\mathbf{u}\cdot \boldsymbol{I}_1)^2 \\
& + \Big[5(A_2 - 2B_2 + C_2)(B_1 - C_1) \\
& \qquad - m_2(5Z_1 + \frac{20}{3}Y_1 - 35P_1 + 5Q_1 - 5R_1)\Big](\mathbf{u}\cdot \boldsymbol{K}_1)^2 \\
& + \Big[5(A_1 - 2B_1 + C_1)(B_2 - A_2) \\
& \qquad - m_1(5X_2 + \frac{20}{3}Y_2 - 5P_2 + 5Q_2 - 35R_2)\Big](\mathbf{u}\cdot \boldsymbol{I}_2)^2 \\
& + \Big[5(A_1 - 2B_1 + C_1)(B_2 - C_2) \\
& \qquad - m_1(5Z_2 + \frac{20}{3}Y_2 - 35P_2 + 5Q_2 - 5R_2)\Big](\mathbf{u}\cdot \boldsymbol{K}_2)^2 \\
& - 20\Big[(B_1 - A_1)(\mathbf{u}\cdot \boldsymbol{I}_1)\boldsymbol{I}_1 + (B_1 - C_1)(\mathbf{u}\cdot \boldsymbol{K}_1)\boldsymbol{K}_1\Big] \\
& \qquad \times \Big[(B_2 - A_2)(\mathbf{u}\cdot \boldsymbol{I}_2)\boldsymbol{I}_2 + (B_2 - C_2)(\mathbf{u}\cdot \boldsymbol{K}_2)\boldsymbol{K}_2\Big] \\
& \qquad + \frac{35}{6}m_2\Big[(X_1 + Y_1 - 6R_1)(\mathbf{u}\cdot \boldsymbol{I}_1)^4 + (Z_1 + Y_1 - 6P_1)(\mathbf{u}\cdot \boldsymbol{K}_1)^4 \\
& \qquad\quad + 2(Y_1 - 3P_1 + 3Q_1 - 3R_1)(\mathbf{u}\cdot \boldsymbol{I}_1)^2(\mathbf{u}\cdot \boldsymbol{K}_1)^2\Big] \\
& \qquad + \frac{35}{6}m_1\Big[(X_2 + Y_2 - 6R_2)(\mathbf{u}\cdot \boldsymbol{I}_2)^4 + (Z_2 + Y_2 - 6P_2)(\mathbf{u}\cdot \boldsymbol{K}_2)^4 \\
& \qquad\quad + 2(Y_2 - 3P_2 + 3Q_2 - 3R_2)(\mathbf{u}\cdot \boldsymbol{I}_2)^2(\mathbf{u}\cdot \boldsymbol{K}_2)^2\Big] \\
& + 35\Big[(B_1 - A_1)(\mathbf{u}\cdot \boldsymbol{I}_1)^2 + (B_1 - C_1)(\mathbf{u}\cdot \boldsymbol{K}_1)^2\Big] \\
& \qquad \times \Big[(B_2 - A_2)(\mathbf{u}\cdot \boldsymbol{I}_2)^2 + (B_2 - C_2)(\mathbf{u}\cdot \boldsymbol{K}_2)^2\Big]\Bigg\}. \qquad (14)
\end{aligned}
$$

The full Hamiltonian (7, 2, 12, 13 and 14) together with the equations of motion (cf section 2.1) enable the integration of the system. The evolution of this system contains fast motions like the rotation of each body around their axis or the orbital revolution. In comparison, the two spin axes as well as the orientation of the orbital plane undergo secular evolutions. In the following, fast motions are averaged in the purpose of studying the long term evolution only.

2.4 Averaging

In this section, we average the Hamiltonian independently over all fast angles: proper rotations and orbital motion. Although this method is strictly valid for non resonant cases only, we will show (in section 6) an application to a typical primary-asynchronous, secondary-synchronous binary asteroid system where the motion is regular. The method still gives very acceptable results. In the following, we forget the subscripts 1 and 2 whenever we consider any of the two bodies without distinction.

To average over proper rotations, Andoyer variables (G, H, L, g, h, l) as described in Fig. (2) are well suited. In a first step, the dependency of the full Hamiltonian on $\boldsymbol{I}_1$ and $\boldsymbol{I}_2$ is removed by averaging over l_1 and l_2. We have

$$\boldsymbol{I} = \left(\begin{array}{c} \cos l \\ \sin l \\ 0 \end{array} \right)_{(\boldsymbol{n},\boldsymbol{n}',\boldsymbol{K})} \tag{15}$$

where $\boldsymbol{n}$ is defined in Fig. (2) and $\boldsymbol{n}' = \boldsymbol{K} \times \boldsymbol{n}$. The vectors $\boldsymbol{n}$, $\boldsymbol{n}'$ and $\boldsymbol{K}$ are independent of l, thus

$$\begin{aligned} \langle \boldsymbol{I} \rangle_l &= \boldsymbol{0} \ ; \\ \left\langle \boldsymbol{I}^t \boldsymbol{I} \right\rangle_l &= \frac{1}{2}(Id - \boldsymbol{K}^t \boldsymbol{K}) \ ; \\ \left\langle (\boldsymbol{s}\cdot \boldsymbol{I})^4 \right\rangle_l &= \frac{3}{8} \left[\boldsymbol{s}^2 - (\boldsymbol{s}\cdot \boldsymbol{K})^2 \right]^2 \ , \end{aligned} \tag{16}$$

where $\boldsymbol{s}$ is again any vector. After this averaging, the Hamiltonian of the free rotation becomes

$$\langle H_E\rangle_{l_1,l_2} = \frac{\boldsymbol{G}_1^2}{2A'_1} + \left(\frac{1}{C_1} - \frac{1}{A'_1}\right)\frac{(\boldsymbol{G}_1\cdot\boldsymbol{K}_1)^2}{2} + \frac{\boldsymbol{G}_2^2}{2A'_2} + \left(\frac{1}{C_2} - \frac{1}{A'_2}\right)\frac{(\boldsymbol{G}_2\cdot\boldsymbol{K}_2)^2}{2} \quad (17)$$

where

$$\frac{1}{A'} = \frac{1}{2}\left(\frac{1}{A} + \frac{1}{B}\right). \quad (18)$$

And the second and the fourth order terms of the interaction

$$\left\langle H_I^{(2)}\right\rangle_{l_1,l_2} = -\frac{\mathcal{G}\mathcal{C}_1 m_2}{2r^3}\left[1 - 3(\mathbf{u}\cdot\boldsymbol{K}_1)^2\right] - \frac{\mathcal{G}\mathcal{C}_2 m_1}{2r^3}\left[1 - 3(\mathbf{u}\cdot\boldsymbol{K}_2)^2\right], \quad (19)$$

$$\begin{aligned}\left\langle H_I^{(4)}\right\rangle_{l_1,l_2} = &-\frac{3}{8}\frac{\mathcal{G}m_2\mathcal{D}_1}{r^5}\left[1 - 10(\mathbf{u}\cdot\boldsymbol{K}_1)^2 + \frac{35}{3}(\mathbf{u}\cdot\boldsymbol{K}_1)^4\right]\\ &-\frac{3}{8}\frac{\mathcal{G}m_1\mathcal{D}_2}{r^5}\left[1 - 10(\mathbf{u}\cdot\boldsymbol{K}_2)^2 + \frac{35}{3}(\mathbf{u}\cdot\boldsymbol{K}_2)^4\right]\\ &-\frac{3}{4}\frac{\mathcal{G}\mathcal{C}_1\mathcal{C}_2}{r^5}\Big[1 + 2(\boldsymbol{K}_1\cdot\boldsymbol{K}_2)^2 - 5(\mathbf{u}\cdot\boldsymbol{K}_1)^2\\ &-5(\mathbf{u}\cdot\boldsymbol{K}_2)^2 - 20(\mathbf{u}\cdot\boldsymbol{K}_1)(\mathbf{u}\cdot\boldsymbol{K}_2)(\boldsymbol{K}_1\cdot\boldsymbol{K}_2)\\ &+35(\mathbf{u}\cdot\boldsymbol{K}_1)^2(\mathbf{u}\cdot\boldsymbol{K}_2)^2\Big],\end{aligned} \quad (20)$$

where $\mathcal{C} = C - (A+B)/2$ and

$$\mathcal{D} = \frac{3}{8}(X+Y) + Z - 3(P+Q) + \frac{3}{4}R. \quad (21)$$

In a next step, the averaging over the angle g is performed. This corresponds to the averaging of $\boldsymbol{K}$ around $\mathbf{w} = \boldsymbol{G}/G$ (cf Fig. 2). Indeed, in the general case the angular momentum $\boldsymbol{G}$ is not aligned with the axis of maximum inertia $\boldsymbol{K}$, which is implicitly assumed in the gyroscopic approximation. Instead, if there is an angle J between these two vectors then

$$\boldsymbol{K} = \begin{pmatrix}\sin J\sin g\\ -\sin J\cos g\\ \cos J\end{pmatrix}_{(\mathbf{N_1},\mathbf{U_1},\mathbf{w})} \quad (22)$$

where $\mathbf{N}_1$ is defined in Fig. 2 and $\mathbf{U_1} = \mathbf{w} \times \mathbf{N_1}$. The vectors $\mathbf{N}_1$, $\mathbf{U_1}$ and $\mathbf{w}$ are independent of g, so

$$\begin{aligned}
\langle \boldsymbol{K} \rangle_g &= (\cos J)\mathbf{w} \ ; \\
\left\langle \boldsymbol{K}^t \boldsymbol{K} \right\rangle_g &= \frac{1}{2}(\sin^2 J) Id + \left(1 - \frac{3}{2}\sin^2 J\right) \mathbf{w}^t \mathbf{w} \ ; \\
\left\langle (\boldsymbol{s}\cdot \boldsymbol{K})^4 \right\rangle_g &= \left(1 - 5\sin^2 J + \frac{35}{8}\sin^4 J\right)(\boldsymbol{s}\cdot \mathbf{w})^4 \\
&\quad + 3\sin^2 J \left(1 - \frac{5}{4}\sin^2 J\right) \boldsymbol{s}^2 (\boldsymbol{s}\cdot \mathbf{w})^2 \\
&\quad + \frac{3}{8}\sin^4 J \boldsymbol{s}^4 \ ,
\end{aligned} \tag{23}$$

where $\boldsymbol{s}$ is any vector. After averaging over g_1 and g_2, the conjugated momenta G_1 and G_2 become constant. The averaged Euler Hamiltonian which depends only on G_1 and G_2

$$\begin{aligned}
\langle H_E \rangle_{l,g} = &\left(\frac{\cos^2 J_1}{C_1} + \frac{\sin^2 J_1}{A'_1}\right)\frac{\boldsymbol{G}_1^2}{2} \\
&+ \left(\frac{\cos^2 J_2}{C_2} + \frac{\sin^2 J_2}{A'_2}\right)\frac{\boldsymbol{G}_2^2}{2}
\end{aligned} \tag{24}$$

is now a constant and can be ignored. In this expression, A' is still the harmonic mean of A and B (18). The only change in the interaction is the substitution of $\mathcal{C}$ and $\mathcal{D}$ in (19-20) by

$$\begin{aligned}
\mathcal{C}' &= \left(1 - \frac{3}{2}\sin^2 J\right)\mathcal{C} \\
\mathcal{D}' &= \left(1 - 5\sin^2 J + \frac{35}{8}\sin^4 J\right)\mathcal{D}
\end{aligned} \tag{25}$$

and $(\boldsymbol{K}_1, \boldsymbol{K}_2)$ by $(\mathbf{w}_1, \mathbf{w}_2)$. For fast rotating non-rigid bodies, the angle J is assumed to be very small as a result of internal dissipation ($J \approx 10^{-7}$ radians for the Earth). In that case, the gyroscopic approximation $J = 0$ is a good approximation since the correction obtained after averaging over fast angles is in $O(\sin^2 J)$. Nevertheless, for slow rotating triaxial asteroids, the angle J may be large and the gyroscopic approximation may not be valid.

In a third step the Hamiltonian is averaged over the orbital motion. First over the mean anomaly M, and then over the longitude of periapse ω. The first average is computed using the formulas of the Appendix C and for the second one, we have similar equations as (16)

$$\begin{aligned} \langle \boldsymbol{I} \rangle_{\omega} &= \mathbf{0} \; ; \\ \left\langle \boldsymbol{I}^t \boldsymbol{I} \right\rangle_{\omega} &= \frac{1}{2}(Id - \mathbf{w}^t \mathbf{w}) \; ; \\ \left\langle (\boldsymbol{s} \cdot \boldsymbol{I})^4 \right\rangle_{\omega} &= \frac{3}{8} \left[\boldsymbol{s}^2 - (\boldsymbol{s} \cdot \mathbf{w})^2 \right]^2 \; , \end{aligned} \tag{26}$$

where $\boldsymbol{I}$ now denotes direction of the periapse and $\mathbf{w}$ the normal of the orbit. The resulting secular Hamiltonian $H_s = \langle \mathcal{H} \rangle_{l_1, l_2, g_1, g_2, M, \omega}$ is thus

$$\begin{aligned} H_s = & \left(\frac{\cos^2 J_1}{C_1} + \frac{\sin^2 J_1}{A'_1} \right) \frac{\boldsymbol{G}_1^2}{2} + \left(\frac{\cos^2 J_2}{C_2} + \frac{\sin^2 J_2}{A'_2} \right) \frac{\boldsymbol{G}_2^2}{2} \\ & - \frac{\mu \beta}{2a} \\ & + \frac{\mathcal{G}}{4a^3 (1-e^2)^{3/2}} \left[m_2 \mathcal{C}'_1 (1 - 3x^2) + m_1 \mathcal{C}'_2 (1 - 3y^2) \right] \\ & - \frac{9}{32} \frac{\mathcal{G}}{a^5 (1-e^2)^{7/2}} \left(1 + \frac{3}{2} e^2 \right) \Bigg[\\ & \mathcal{C}'_1 \mathcal{C}'_2 (1 - 5x^2 - 5y^2 + 2z^2 - 20xyz + 35x^2 y^2) \\ & + \frac{m_2 \mathcal{D}'_1}{2} \left(1 - 10x^2 + \frac{35}{3} x^4 \right) \\ & + \frac{m_1 \mathcal{D}'_2}{2} \left(1 - 10y^2 + \frac{35}{3} y^4 \right) \Bigg] \end{aligned} \tag{27}$$

where $x = (\mathbf{w} \cdot \mathbf{w}_1)$, $y = (\mathbf{w} \cdot \mathbf{w}_2)$ and $z = (\mathbf{w}_1 \cdot \mathbf{w}_2)$. Let us write H_s in the more compact form

$$H_s = -\frac{\mathfrak{a}}{2} x^2 - \frac{\mathfrak{b}}{2} y^2 - \frac{\mathfrak{c}}{2} z^2 + \mathfrak{d} xyz - \frac{\mathfrak{e}}{4} x^4 - \frac{\mathfrak{f}}{4} y^4 - \frac{\mathfrak{g}}{2} x^2 y^2 + \mathfrak{h} \tag{28}$$

where

$$
\begin{aligned}
\mathfrak{a} &= k_3 m_2 \mathcal{C}_1' - \frac{5}{2} k_5 (\mathcal{C}_1' \mathcal{C}_2' + m_2 \mathcal{D}_1') \\
\mathfrak{b} &= k_3 m_1 \mathcal{C}_2' - \frac{5}{2} k_5 (\mathcal{C}_1' \mathcal{C}_2' + m_1 \mathcal{D}_2') \\
\mathfrak{c} &= k_5 \mathcal{C}_1' \mathcal{C}_2' \\
\mathfrak{d} &= 5 k_5 \mathcal{C}_1' \mathcal{C}_2' \\
\mathfrak{e} &= \frac{35}{6} k_5 m_2 \mathcal{D}_1' \\
\mathfrak{f} &= \frac{35}{6} k_5 m_1 \mathcal{D}_2' \\
\mathfrak{g} &= \frac{35}{2} k_5 \mathcal{C}_1' \mathcal{C}_2' \\
\mathfrak{h} &= \frac{1}{6} k_3 (m_2 \mathcal{C}_1' + m_1 \mathcal{C}_2') - \frac{1}{8} k_5 (2 \mathcal{C}_1' \mathcal{C}_2' + m_2 \mathcal{D}_1' + m_1 \mathcal{D}_2') \\
&\quad + \langle H_E \rangle_{l,g} - \frac{\mu \beta}{2a}
\end{aligned}
\tag{29}
$$

with

$$
\begin{aligned}
k_3 &= \frac{3}{2} \frac{\mathcal{G}}{a^3 (1-e^2)^{3/2}} \\
k_5 &= \frac{9}{8} \frac{\mathcal{G}}{a^5 (1-e^2)^{7/2}} \left(1 + \frac{3}{2} e^2 \right).
\end{aligned}
\tag{30}
$$

3 Secular equations

The secular Hamiltonian H_s (28) is similar to the one obtained in BL06 although its expression is slightly more complicated. The difference with BL06 is that the secular Hamiltonian is not anymore the equation of an ellipsoid in (x, y, z). A few results in BL06 were proved for this special surface. We recall here the main steps of the derivation of the solutions adapted to the

new surface defined by the current secular Hamiltonian.

The Hamiltonian H_s is only a function of the angular momenta $(\boldsymbol{G}, \boldsymbol{G}_1, \boldsymbol{G}_2)$. The equations of motion of these quantities are

$$\begin{aligned} \dot{\boldsymbol{G}} &= \boldsymbol{\nabla}_{\boldsymbol{G}} H_s \times \boldsymbol{G} \ , \\ \dot{\boldsymbol{G}}_1 &= \boldsymbol{\nabla}_{\boldsymbol{G}_1} H_s \times \boldsymbol{G}_1 \ , \\ \dot{\boldsymbol{G}}_2 &= \boldsymbol{\nabla}_{\boldsymbol{G}_2} H_s \times \boldsymbol{G}_2 \ . \end{aligned} \tag{31}$$

We thus have $\boldsymbol{G}\cdot\dot{\boldsymbol{G}} = \boldsymbol{G}_1\cdot\dot{\boldsymbol{G}}_1 = \boldsymbol{G}_2\cdot\dot{\boldsymbol{G}}_2 = 0$ which means that the norms $\gamma = \|\boldsymbol{G}\|$, $\beta = \|\boldsymbol{G}_1\|$ and $\alpha = \|\boldsymbol{G}_2\|$ are constant. It is thus possible to write the general equations directly in terms of the unit vectors $(\mathbf{w}, \mathbf{w}_1, \mathbf{w}_2)$

$$\begin{aligned} \dot{\mathbf{w}} &= \frac{1}{\gamma}\boldsymbol{\nabla}_{\mathbf{w}} H_s \times \mathbf{w} \ , \\ \dot{\mathbf{w}}_1 &= \frac{1}{\beta}\boldsymbol{\nabla}_{\mathbf{w}_1} H_s \times \mathbf{w}_1 \ , \\ \dot{\mathbf{w}}_2 &= \frac{1}{\alpha}\boldsymbol{\nabla}_{\mathbf{w}_2} H_s \times \mathbf{w}_2 \ . \end{aligned} \tag{32}$$

From the expression of the secular Hamiltonian (28), we get

$$\begin{aligned} \dot{\mathbf{w}} &= -\frac{p}{\gamma}\mathbf{w}_1 \times \mathbf{w} - \frac{q}{\gamma}\mathbf{w}_2 \times \mathbf{w} \ , \\ \dot{\mathbf{w}}_1 &= -\frac{p}{\beta}\mathbf{w} \times \mathbf{w}_1 - \frac{s}{\beta}\mathbf{w}_2 \times \mathbf{w}_1 \ , \\ \dot{\mathbf{w}}_2 &= -\frac{q}{\alpha}\mathbf{w} \times \mathbf{w}_2 - \frac{s}{\alpha}\mathbf{w}_1 \times \mathbf{w}_2 \ , \end{aligned} \tag{33}$$

where

$$\begin{aligned} p &= \mathfrak{a}x - \mathfrak{d}yz + \mathfrak{e}x^3 + \mathfrak{g}xy^2 \ , \\ q &= \mathfrak{b}y - \mathfrak{d}xz + \mathfrak{f}y^3 + \mathfrak{g}x^2y \ , \\ s &= \mathfrak{c}z - \mathfrak{d}xy \ . \end{aligned} \tag{34}$$

The problem has 9 degrees of freedom, the coordinates of $\boldsymbol{G}$, $\boldsymbol{G}_1$ and $\boldsymbol{G}_2$, and the equations

(33-34) are non-linear. At first glance the resolution is difficult. There are 7 first integrals

$$\begin{aligned}
&\|\mathbf{w}\| = 1 \\
&\|\mathbf{w}_1\| = 1 \\
&\|\mathbf{w}_2\| = 1 \\
&\mathfrak{a}x^2 + \mathfrak{b}y^2 + \mathfrak{c}z^2 - 2\mathfrak{d}xyz + \frac{\mathfrak{e}}{2}x^4 + \frac{\mathfrak{f}}{2}y^4 + \mathfrak{g}x^2y^2 = -2H_s \\
&\gamma\mathbf{w} + \beta\mathbf{w}_1 + \alpha\mathbf{w}_2 = \boldsymbol{W}_0
\end{aligned} \tag{35}$$

where $\boldsymbol{W}_0$ is the total angular momentum. Thus one misses one constant of motion to integrate the problem by quadrature. The next section shows how to solve the relative motion of the three vectors that contains enough constants of motion.

3.1 Relative solution

In the previous section, we have shown that the number of first integrals is not large enough to solve the full problem. But the number of degrees of freedom can be decreased by considering only the relative distance between the vectors. These distances are given by the dot products $x = \mathbf{w}\cdot\mathbf{w}_1$, $y = \mathbf{w}\cdot\mathbf{w}_2$ and $z = \mathbf{w}_1\cdot\mathbf{w}_2$. From the equations (33), one can derive the new equations of motion

$$\begin{aligned}
\dot{x} &= \left(-\frac{q}{\gamma} + \frac{s}{\beta}\right) v \ , \\
\dot{y} &= \left(-\frac{s}{\alpha} + \frac{p}{\gamma}\right) v \ , \\
\dot{z} &= \left(-\frac{p}{\beta} + \frac{q}{\alpha}\right) v \ .
\end{aligned} \tag{36}$$

where $v = (\mathbf{w}\times\mathbf{w}_1)\cdot\mathbf{w}_2$ is the volume defined by the 3 vectors. It can be expressed in terms of x, y and z through the Gram determinant

$$v^2 = \begin{vmatrix} 1 & x & y \\ x & 1 & z \\ y & z & 1 \end{vmatrix} = 1 - x^2 - y^2 - z^2 + 2xyz. \tag{37}$$

This restricted problem has only 3 degrees of freedom and 2 first integrals

$$\begin{aligned} &\mathfrak{a}x^2 + \mathfrak{b}y^2 + \mathfrak{c}z^2 - 2\mathfrak{d}xyz + \frac{\mathfrak{e}}{2}x^4 + \frac{\mathfrak{f}}{2}y^4 + \mathfrak{g}x^2y^2 = -2H_s \\ &\gamma\beta x + \alpha\gamma y + \alpha\beta z = K \end{aligned} \tag{38}$$

the second integral being simply derived from $2K = \|\boldsymbol{W}_0\|^2 - (\gamma^2 + \beta^2 + \alpha^2)$. The motion in (x, y, z) is thus integrable and the solution evolves in the intersection $\mathscr{C}$ of the quartic $H_s = Cte$ and the plane $K = Cte$ [2]. Moreover, the evolution is limited to the interior of the $v^2(x, y, z) = 0$ surface that will be henceforth called the Cassini berlingot[3] as in BL06 (cf Fig. 3). Outside this surface we would have $v^2 < 0$ which is not possible (see BL06).

3.1.1 Shape of the quartic surface

The constraint $H_s = Cte$ defines a quartic surface $\mathcal{Q}$ in (x, y, z). Quartic surfaces can have very different shapes, nevertheless setting $z' = z - \frac{\mathfrak{d}}{\mathfrak{c}}xy$, one obtains

$$-2H_s = \mathfrak{a}x^2 + \mathfrak{b}y^2 + \mathfrak{c}z'^2 + \frac{\mathfrak{e}}{2}x^4 + \frac{\mathfrak{f}}{2}y^4 + \left(\mathfrak{g} - \frac{\mathfrak{d}^2}{\mathfrak{c}}\right)x^2y^2 \tag{39}$$

which is a biquadratic. The new surface $\mathcal{Q}'$ defined by (39) is thus symmetric in x, y and z'. In (x^2, y^2, z') the surface $\mathcal{Q}'$ can be either an ellipsoid, a paraboloid or an hyperboloid depending on the sign of

$$\delta = \mathfrak{e}\mathfrak{f} - \left(\mathfrak{g} - \frac{\mathfrak{d}^2}{\mathfrak{c}}\right)^2. \tag{40}$$

If $\delta > 0$ then it is an ellipsoid and x, y, z' and thus z are bounded. In the other case, $\mathcal{Q}'$ is either an elliptic paraboloid if $\delta = 0$ or an hyperboloid of one or two sheets depending on the value of H_s if $\delta < 0$. Thus, x, y, z are unbounded.

From the definition of the coefficients $\mathfrak{a}$–$\mathfrak{g}$ (29), δ can be rewritten in the following form

$$\delta = \left(\frac{35}{6}\right)^2 k_5^2 m_1 m_2 \mathcal{D}_1' \mathcal{D}_2' - \left(\frac{15}{2}\right)^2 k_5^2 \mathcal{C}_1'^2 \mathcal{C}_2'^2. \tag{41}$$

[2] In the whole paper, Cte means any constant value.

[3] A berlingot is a famous tetrahedron hard candy with rounded edges.

Using the definition of the coefficients $\mathcal{C}'$ and $\mathcal{D}'$ (25) and (21), we get

$$\begin{aligned}\delta = \left(\frac{15}{2}\right)^2 k_5^2 \mathcal{C}_1^2 \mathcal{C}_2^2 \Bigg[& \\ & \eta \left(1 - 5\sin^2 J_1 + \frac{35}{8}\sin^4 J_1\right) \\ & \times \left(1 - 5\sin^2 J_2 + \frac{35}{8}\sin^4 J_2\right) \\ & - \left(1 - \frac{3}{2}\sin^2 J_1\right)^2 \left(1 - \frac{3}{2}\sin^2 J_2\right)^2 \Bigg]\end{aligned} \tag{42}$$

where η is a positive parameter related to the shapes of the rigid bodies

$$\eta = \left(\frac{7}{9}\right)^2 \frac{m_1 \mathcal{D}_1 m_2 \mathcal{D}_2}{\mathcal{C}_1^2 \mathcal{C}_2^2} \ . \tag{43}$$

Let us look to the range of the possible values of η in the case of an homogeneous ellipsoids. We have the relation between $\mathcal{D}$ and $\mathcal{C}$ given by the equations (9)

$$\mathcal{D} = \frac{15}{7m}\left[\mathcal{C}^2 + \frac{1}{8}(B-A)^2\right] \ . \tag{44}$$

The lowest value of η is thus obtained for $A = B$, i.e. for axisymmetric bodies. In that case, $\eta_{\min} = 25/9$. Conversely, the largest value of η is attained when $(B-A)^2$ is maximal, thus when $B = C$ and $A = 0$, that is, in the limiting case where the bodies are extremly thin rods. In this second case, $\eta_{\max} = 25/4$. So, for homogeneous ellipsoids, η is constrained between $\eta_{\min}$ and $\eta_{\max}$.

Figure 4 shows the domains where the surface $\mathcal{Q}'$ is an ellipsoid ($\mathcal{E}$) or an hyperboloid ($\mathcal{H}$) as a function of the angles J_1 and J_2. The two sets of curve correspond to $\eta = \eta_{\min}$ and $\eta = \eta_{\max}$. As δ is a function of $\sin^2 J_1$ and $\sin^2 J_2$, the figure can be extended up to 180 degrees applying axial symmetry around the axis $J_1 = 90$ degrees and $J_2 = 90$ degrees.

3.1.2 Description of the solutions

In BL06, we show that when the surface $\mathcal{Q}$ is an ellipsoid then the evolution of (x, y, z) presents two kinds of solutions. We have called *special solutions* the solutions where $\mathscr{C}$ is totally included

in the Cassini berlingot $\mathcal{B}$. This means that the vectors $\mathbf{w}$, $\mathbf{w}_1$ and $\mathbf{w}_2$ are never collinear. This happens only when the three vectors are almost orthogonal. The second class of solutions are the *general solutions*, more frequent in astronomical problems, for which $\mathscr{C}$ crosses the Cassini berlingot (Fig. 5). In that case $\boldsymbol{M} = (x, y, z)$ does periodic returns inside the Cassini berlingot up to its surface and the volume v defined by the three vectors $\mathbf{w}$, $\mathbf{w}_1$ and $\mathbf{w}_2$ is conserved over one period. In both cases, solutions are periodic.

There are also special cases that happen when the orbit of (x, y, z) is tangent to the Cassini berlingot. At the tangency there is indeed a fixed point. In that state, the three vectors remain in a plane that precesses in time. It is called a Cassini state (Colombo, 1966; Peale, 1969; Ward, 1975; BL06). If an initial condition is chosen along such special orbits but strictly outside the fixed point, then the system cannot reach the stationary point in finite time and it is the only case where x, y, z are not periodic.

Here, we have the same results except when the quartic $\mathcal{Q}$ is unbounded. In that case, we cannot have special solutions.

3.2 Global solution

Knowing that x, y, z are periodic functions of time, it is possible to get general features of the global motion. For that, let us rewrite the secular equations (33) in a new form so as to obtain a linear differential system with periodic coefficients.

Let us assume as in BL06 that the vectors $(\mathbf{w}, \mathbf{w}_1, \mathbf{w}_2)$ are not coplanar ($v \neq 0$). Let $\mathcal{W}$ be the matrix $(\mathbf{w}, \mathbf{w}_1, \mathbf{w}_2)$ and V the Gram matrix of the basis $(\mathbf{w}, \mathbf{w}_1, \mathbf{w}_2)$

$$V = \begin{pmatrix} 1 & x & y \\ x & 1 & z \\ y & z & 1 \end{pmatrix} . \tag{45}$$

Using the expression of the wedge product in the basis $(\mathbf{w}, \mathbf{w}_1, \mathbf{w}_2)$ (see the appendix B of BL06), the equations of motion (33) can be written in the following form

$$\dot{\mathcal{W}} = vV^{-1}\mathcal{W}\mathcal{A}. \tag{46}$$

Here we correct a mistake[4] in the demonstration of the proposition 1, given in section 4 in BL06 (see the erratum Boué and Laskar, 2008).

In (46), vV^{-1} and $\mathcal{A}$ are matrices depending only on (x, y, z) that are periodic functions of period T. Indeed

$$\mathcal{A} = \begin{pmatrix} 0 & \frac{s}{\beta} & -\frac{s}{\alpha} \\ -\frac{q}{\gamma} & 0 & \frac{q}{\alpha} \\ \frac{p}{\gamma} & -\frac{p}{\beta} & 0 \end{pmatrix} \tag{47}$$

and

$$V^{-1} = \frac{1}{v^2} \begin{pmatrix} 1-z^2 & yz-x & xz-y \\ yz-x & 1-y^2 & xy-z \\ xz-y & xy-z & 1-x^2 \end{pmatrix} . \tag{48}$$

Thus, if $\mathcal{W}(t)$ is a solution of (46), then $\mathcal{W}(t+T)$ is also a solution. Let us denote

$$\mathcal{R}_T(t) = \mathcal{W}(t+T)\mathcal{W}(t)^{-1} . \tag{49}$$

We need to prove that $\mathcal{R}_T(t)$ is constant with t. As the Gram matrix V of the vectors $(\mathbf{w}(t), \mathbf{w}_1(t), \mathbf{w}_2(t))$ is T-periodic, the norm is conserved by linear transformation $\mathcal{R}_T(t)$ that send $\mathcal{W}(t)$ into $\mathcal{W}(t+T)$, and $\mathcal{R}(t)$ is thus an isometry of $\mathbb{R}^3$. Moreover, this isometry is positive, as the volume v is conserved over a full period T (see section 3.1.2). The invariance of the total angular momentum $\boldsymbol{W}_0$ (35) then implies that $\mathcal{R}_T(t)$ is a rotation matrix of axis $\boldsymbol{W}_0$.

As $\mathcal{R}_T(t)$ is a rotation in $\mathbb{R}^3$, we have for all $\mathbf{w}_i, \mathbf{w}_j$ in $\{\mathbf{w}, \mathbf{w}_1, \mathbf{w}_2\}$,

$$\begin{aligned} \mathbf{w}_i(t+T) \times \mathbf{w}_j(t+T) &= (\mathcal{R}_T(t)\mathbf{w}_i(t)) \times (\mathcal{R}_T(t)\mathbf{w}_j(t)) \\ &= \mathcal{R}_T(t)(\mathbf{w}_i(t) \times \mathbf{w}_j(t)) . \end{aligned} \tag{50}$$

From the equations of motion (33), we can thus derive

$$\dot{\mathcal{W}}(t+T) = \mathcal{R}_T(t)\dot{\mathcal{W}}(t) . \tag{51}$$

[4]In BL06, we have incorrectly stated that the averaged differential system (51) could be written as $\dot{\mathcal{W}} = \mathcal{W}\mathcal{B}$ where $\mathcal{B} = vV^{-1}\mathcal{A}$ is a matrix depending only on (x, y, z). In fact the correct expression is $\dot{\mathcal{W}} = vV^{-1}\mathcal{W}\mathcal{A}$. In BL06, the proof following the equation (51) has to be modified. This is done in the present paper. The results remain identical.

On the other hand, as $\mathcal{W}(t+T) = \mathcal{R}_T(t)\mathcal{W}(t)$ (49), we deduce that for all t,

$$\dot{\mathcal{R}}_T(t)\mathcal{W}(t) = 0 \ . \tag{52}$$

$\mathcal{R}_T(t)$ is thus a constant matrix $\mathcal{R}_T$. Now, let us denote $\mathcal{R}(t)$ the rotation of axis $\boldsymbol{W}_0$ and angle $t\theta_T/T$ (i.e. $\mathcal{R}(T) = \mathcal{R}_T$). We have

Proposition 1 *The complete solution $\mathcal{W}(t)$ can be expressed on the form*

$$\mathcal{W}(t) = \mathcal{R}(t)\tilde{\mathcal{W}}(t) \ , \tag{53}$$

where $\tilde{\mathcal{W}}(t)$ is periodic with period T, and $\mathcal{R}(t)$ a uniform rotation of axis $\boldsymbol{W}_0$ and angle $t\theta_T/T$. The motion has two periods: the (usually) short period T and the precession period

$$T' = \frac{2\pi}{\theta_T} T \ . \tag{54}$$

3.3 Properties of the solution

A more precise result on the periodic loops can be proved. But before, one needs to write the instantaneous precession speed as a function of (x, y, z).

3.3.1 Instantaneous precession rate

Let us write the time derivative of the precession angle of $\mathbf{w}$ as a function of (x, y, z). The expressions for the other vectors can be obtained in the same way. The following approach is highly inspired by BL06. We set $W_0 = \|\boldsymbol{W}_0\|$ the norm of the total angular momentum and $\mathbf{w}_0 = \boldsymbol{W}_0/W_0$ its direction vector. With

$$\zeta = \mathbf{w} \cdot \mathbf{w}_0, \tag{55}$$

the projection $\mathbf{L}$ of $\mathbf{w}$ on the plane orthogonal to $\mathbf{w}_0$ is

$$\mathbf{L} = \mathbf{w} - \zeta \mathbf{w}_0. \tag{56}$$

Assuming $\mathbf{w} \neq \mathbf{w}_0$, we get $\zeta < 1$. With $L = \|\mathbf{L}\|$, the expression of $\mathbf{L}$ gives

$$L = \sqrt{1-\zeta^2} \qquad \text{and} \qquad \dot{L} = -\frac{\zeta\dot{\zeta}}{\sqrt{1-\zeta^2}}. \tag{57}$$

Moreover, setting $\boldsymbol{\ell} = \mathbf{L}/L$, we get

$$\mathbf{L} = L\boldsymbol{\ell} \qquad \text{and} \qquad \dot{\mathbf{L}} = \dot{L}\boldsymbol{\ell} + \dot{\theta}(\mathbf{w}_0 \times \mathbf{L}) \tag{58}$$

which yields to

$$\dot{\mathbf{L}}^2 = \dot{L}^2 + \dot{\theta}^2(\mathbf{w}_0 \times \mathbf{L})^2 = \dot{L}^2 + \dot{\theta}^2(1-\zeta^2). \tag{59}$$

Now, from the expression of $\mathbf{L}$ (56), we can also write

$$\dot{\mathbf{L}} = \dot{\mathbf{w}} - \dot{\zeta}\mathbf{w}_0 \qquad \text{and} \qquad \dot{\mathbf{L}}^2 = \dot{\mathbf{w}}^2 - \dot{\zeta}^2. \tag{60}$$

Finally, we have

$$\dot{\theta}^2 = \frac{\dot{\mathbf{w}}^2 - \dot{\zeta}^2/(1-\zeta^2)}{1-\zeta^2}. \tag{61}$$

This final expression is an explicit function of (x, y, z). Indeed, from (35), one has

$$\zeta = \frac{1}{W_0}(\gamma + \beta x + \alpha y) \tag{62}$$

and thus

$$\dot{\zeta} = \frac{v}{W_0}\left(\frac{\alpha p}{\gamma} - \frac{\beta q}{\gamma}\right). \tag{63}$$

We have also from (33)

$$\dot{\mathbf{w}}^2 = \frac{1}{\gamma^2}\left(p^2 + q^2 + 2pqz - (px+qy)^2\right). \tag{64}$$

so (61) can be written on the form

$$\dot{\theta}^2 = \Theta(x, y, z). \tag{65}$$

The sign of $\dot{\theta}$ can be determined through (58). Indeed $\dot{\theta}$ is a function of $(\mathbf{w}, \mathbf{w}_1\mathbf{w}_2)$, but its sign can only change when $\dot{\theta} = 0$, that is from (61), when

$$\dot{\mathbf{w}}^2(1-\zeta^2) = \dot{\zeta}^2. \tag{66}$$

The equation (65) thus gives the instantaneous precession rate of $\mathbf{w}$ as a function of x, y, z. Same results can easily be obtained for the other two vectors $\mathbf{w}_1$ and $\mathbf{w}_2$.

3.3.2 Symmetry of the nutation

It is now possible to prove a more precise result on the periodic loops generated by $\mathbf{w}$, $\mathbf{w}_1$ and $\mathbf{w}_2$ in the precessing frame. This is the same result as in BL06 that was given for a three body problem with only one rigid body.

Proposition 2 *In the frame rotating uniformly with the precession period, the three vectors* $\mathbf{w}$, $\mathbf{w}_1$, $\mathbf{w}_2$ *describe periodic loops* $\mathcal{L}$, $\mathcal{L}_1$, $\mathcal{L}_2$ *that are all symmetric with respect to the same plane* $\mathcal{S}$ *containing* $\mathbf{w}_0$.

Consequence. Let us call $\mathcal{P}$, $\mathcal{P}_1$, $\mathcal{P}_2$ the averages of $\mathbf{w}$, $\mathbf{w}_1$, $\mathbf{w}_2$ over the nutation angle. $\mathcal{P}$, $\mathcal{P}_1$, $\mathcal{P}_2$ are respectively the pole of the orbit, the pole of the spin of the primary and the pole of the spin of the secondary. Due to the symmetry of the loops, the three poles $\mathcal{P}$, $\mathcal{P}_1$ and $\mathcal{P}_2$ remain in the symmetry plane $\mathcal{S}$ containing $\mathbf{w}_0$, and precessing uniformly around $\mathbf{w}_0$. Each vector $\mathbf{w}$, $\mathbf{w}_1$, $\mathbf{w}_2$ nutates around its pole, respectively $\mathcal{P}$, $\mathcal{P}_1$, $\mathcal{P}_2$.

Proof. As in BL06, we will consider uniquely $\mathbf{w}$, the other cases being similar. We consider here a general solution, for which the orbit of (x, y, z) crosses the Cassini berlingot (Fig. 5). We choose the origin of time in τ_+ which corresponds to an orbital angular momentum $\mathbf{w}_+$. Let σ be the arc length described by $\boldsymbol{M} = (x, y, z)$ computed from $\boldsymbol{M}_+ = \boldsymbol{M}(\tau_+)$. From (36) we have

$$\dot{\sigma} = v\sqrt{f(x, y, z)} \tag{67}$$

where

$$f(x, y, z) = \left(\frac{q}{\gamma} - \frac{s}{\beta}\right)^2 + \left(\frac{s}{\alpha} - \frac{p}{\gamma}\right)^2 + \left(\frac{p}{\beta} - \frac{q}{\alpha}\right)^2. \tag{68}$$

$f(x, y, z) = 0$ if and only if $\alpha p = \beta q = \gamma s$. This condition corresponds to a fixed point of the system. Else $f(x, y, z)$ is strictly positive.

Thus $\dot{\sigma}$ is a function of (x, y, z) and has the sign of v. For $t < 0$, the orbit in the (x, y, z) describes the arc (τ_-, τ_+), thus σ decreases from σ_- down to $\sigma_+ = 0$, and $v < 0$. Conversely, for $t > 0$ the orbit describes the same arc in the reverse way (τ_+, τ_-), hence $v > 0$. As x, y, z

are functions of the arc length σ, we can write

$$\dot{\sigma} = \begin{cases} -F(\alpha), & \text{if } t < 0, \\ +F(\alpha), & \text{if } t > 0 \end{cases} \tag{69}$$

where $F(\alpha) = |v|\sqrt{f(x,y,z)}$. We conclude that σ and thus $\boldsymbol{M} = (x,y,z)$ are even, that is $\boldsymbol{M}(-t) = \boldsymbol{M}(t)$.

The rest of the proof is identical to the one of BL06. We recall it for completeness. From (65)

$$\dot{\theta}^2(t) = \Theta(x,y,z), \tag{70}$$

we deduce that $\dot{\theta}^2(t)$ is even. Moreover, as the differential system (33) is polynomial, the solutions $\mathbf{w}$, $\mathbf{w}_1$, $\mathbf{w}_2$ are analytical in time t, and so will be the coordinate angle $\theta(t)$ of $\mathbf{w}$. The lemma of BL06 thus implies that $\dot{\theta}(t)$ is odd or even. If $\dot{\theta}(t)$ is even on $[-T/2, T/2]$, for all $h \in [0, T/2]$, we have $\theta(h) - \theta(0) = \theta(0) - \theta(-h)$. As the cosine ζ of the angle from $\mathbf{w}$ and $\mathbf{w}_0$ (55) depends only on x, y (62), we have $\zeta(h) = \zeta(-h)$, and $\mathbf{w}(h)$ and $\mathbf{w}(-h)$ are symmetrical with respect to the $(\mathbf{w}_0, \mathbf{w}_+)$ plane. It will still be the same in the rotating frame with the precession period. In this rotating frame, the periodic loop generated by $\mathbf{w}$ is thus symmetric with respect to the plane $(\mathbf{w}_0, \mathbf{w}_+)$.

Moreover, at $t = 0$ (τ_+), the volume v is null, and thus $\mathbf{w}_0$, $\mathbf{w}$, $\mathbf{w}_1$, $\mathbf{w}_2$ are coplanar. In the rotating frame, all three orbits generated by $\mathbf{w}$, $\mathbf{w}_1$, $\mathbf{w}_2$ are thus symmetrical with respect to the same plane $(\mathbf{w}_0, \mathbf{w}_+)$.

The only case where $\dot{\theta}(t)$ is odd, occurs when $\dot{\theta}(0) = 0$. As $v(0) = 0$, we have $\dot{\zeta}(0) = \mathbf{0}$ (63) and $\dot{\mathbf{w}} = \mathbf{0}$ (61). In the same way, we have $\dot{\mathbf{w}}_1(0) = \dot{\mathbf{w}}_2(0) = \mathbf{0}$, and the vector field (33) vanishes at $t = 0$. The three vectors $\mathbf{w}$, $\mathbf{w}_1$, $\mathbf{w}_2$ are thus stationary and coplanar.

This is a special Cassini state where the precession frequency is zero.

3.4 Computation of the two periods

The nutation period and the precession period are two key parameters of the problem since the global solution is the product of these two motions (53). Let us see how the values can be

derived.

The three dot products $(x(t), y(t), z(t))$ are T-periodic where T is the nutation period. This period can thus be calculated from the expression of $(x(t), y(t), z(t))$. Given the two first integrals (35), it is possible to express $x(t)$, $y(t)$, and $z(t)$ in the form of an integral as in BL06. Nevertheless the energy conservation only gives an implicit relation between those variables and the computation remains tedious. For this reason, we give here an algorithm that enables to compute the two frequencies in a simple way using the numerical integration of the secular equations (33). The method leads to an arbitrary high precision since it necessitates the integration over one nutation period only.

We assume that at $t_0 = 0$, the initial volume v (36) is not zero, and let x (for example) be the variable with the largest variation rate, $\dot{x}(t_0)$. Using the method of Hénon (1963), we search for the first time $t > t_0$ when $(x(t), \dot{x}(t)) = (x(t_0), \dot{x}(t_0))$. We integrate the system (33) until

$$\begin{cases} x_{n-1} < x_0 \\ x_n \quad \geq x_0 \end{cases} \quad \text{if } \dot{x}(t_0) > 0 \tag{71}$$

or

$$\begin{cases} x_{n-1} > x_0 \\ x_n \quad \leq x_0 \end{cases} \quad \text{if } \dot{x}(t_0) < 0 \ . \tag{72}$$

We then change the time variable to x and integrate

$$\begin{aligned} \frac{dt}{dx} &= \frac{1}{\dot{x}(x,y,z)}, \\ \frac{dy}{dx} &= \frac{\dot{y}(x,y,z)}{\dot{x}(x,y,z)}, \\ \frac{dz}{dx} &= \frac{\dot{z}(x,y,z)}{\dot{x}(x,y,z)}, \\ \frac{d\theta}{dx} &= \frac{\epsilon\sqrt{\Theta(x,y,z)}}{\dot{x}(x,y,z)} \ , \end{aligned} \tag{73}$$

from x_n to x_0. The latter equation comes from (65) and will provide the rotation angle of the vectors over one nutation period (knowing the initial angle $\theta(t_0)$). We thus have the nutation period $t = T$ and $\theta_T = \theta(T) - \theta(t_0)$. The precession period is simply given by

$$T' = \frac{2\pi}{\theta_T} T \ . \tag{74}$$

4 Analytical approximation

In this section we give an analytical approximation of the secular evolution. So far, only general features of the solutions have been obtained. Here analytical approximations of the two frequencies that appear in the problem as well as their amplitudes are computed. The two frequencies being the global precession and the nutation.

In an invariant frame where the third axis is aligned with the direction $\mathbf{w}_0$ of the total angular momentum, we can write

$$\mathbf{w} = \begin{pmatrix} \xi \\ \eta \\ \zeta \end{pmatrix}, \qquad \mathbf{w}_1 = \begin{pmatrix} \xi_1 \\ \eta_1 \\ \zeta_1 \end{pmatrix}, \qquad \mathbf{w}_2 = \begin{pmatrix} \xi_2 \\ \eta_2 \\ \zeta_2 \end{pmatrix} \tag{75}$$

where

$$\zeta = \frac{\gamma + \beta x + \alpha y}{W_0}, \quad \zeta_1 = \frac{\gamma x + \beta + \alpha z}{W_0},$$

$$\zeta_2 = \frac{\gamma y + \beta z + \alpha}{W_0} \ . \tag{76}$$

The evolution of the projections on the complex plane orthogonal to $\mathbf{w}_0$

$$\mathfrak{z} = \xi + i\eta, \quad \mathfrak{z}_1 = \xi_1 + i\eta_1, \quad \mathfrak{z}_2 = \xi_2 + i\eta_2, \tag{77}$$

is obtained from the secular equations (33), and yields to

$$\frac{d}{dt} \begin{pmatrix} \mathfrak{z} \\ \mathfrak{z}_1 \\ \mathfrak{z}_2 \end{pmatrix} = iM \begin{pmatrix} \mathfrak{z} \\ \mathfrak{z}_1 \\ \mathfrak{z}_2 \end{pmatrix} \tag{78}$$

where

$$M = \begin{pmatrix} -\frac{p}{\gamma}\zeta_1 - \frac{q}{\gamma}\zeta_2 & \frac{p}{\gamma}\zeta & \frac{q}{\gamma}\zeta \\ \frac{p}{\beta}\zeta_1 & -\frac{p}{\beta}\zeta - \frac{s}{\beta}\zeta_2 & \frac{s}{\beta}\zeta_1 \\ \frac{q}{\alpha}\zeta_2 & \frac{s}{\alpha}\zeta_2 & -\frac{q}{\alpha}\zeta - \frac{s}{\alpha}\zeta_1 \end{pmatrix} \tag{79}$$

and (p, q, s) are defined in (34). M is a real matrix with periodic coefficients. As it is not possible to obtain a simple analytical solution of this system, we make a crude approximation. Hereafter we replace the matrix M by the constant matrix $\tilde{M}$ obtained by substituting (x, y, z) by their average

$$\tilde{M} = M(\tilde{x}, \tilde{y}, \tilde{z}) \ . \tag{80}$$

The solution of (78) is thus straightforward. It is easy to verify that $(\zeta, \zeta_1, \zeta_2)$ is an eigenvector of $\tilde{M}$ with eigenvalue 0. The other eigenvalues are then the solutions of

$$\lambda^2 - \mathbf{T}\lambda + \mathbf{P} = 0 \tag{81}$$

where $\mathbf{T}$ is the trace of $\tilde{M}$ and

$$\mathbf{P} = \left(\frac{\zeta}{\alpha\beta} + \frac{\zeta_1}{\gamma\alpha} + \frac{\zeta_2}{\beta\gamma}\right)(pq\zeta + sp\zeta_1 + qs\zeta_2) \ . \tag{82}$$

Let Ω and $\Omega + \nu$ be the other two eigenvalues such that

$$\Omega = \frac{\mathbf{T} + \sqrt{\mathbf{T}^2 - 4\mathbf{P}}}{2}, \qquad \nu = -\sqrt{\mathbf{T}^2 - 4\mathbf{P}} \ . \tag{83}$$

The system possesses three eigenmodes

$$\mathfrak{u}e^{i\psi}, \qquad \mathfrak{r}e^{i(\Omega t + \Phi)}, \qquad \mathfrak{s}e^{i[(\Omega+\nu)t + \Phi + \phi]}, \tag{84}$$

with eigenvectors

$$e_0 = \begin{pmatrix} \zeta \\ \zeta_1 \\ \zeta_2 \end{pmatrix}, \qquad e_1 = \begin{pmatrix} 1 \\ \lambda \\ \mu \end{pmatrix}, \qquad e_2 = \begin{pmatrix} 1 \\ \lambda' \\ \mu' \end{pmatrix}, \tag{85}$$

where λ, λ', μ and μ' are real numbers. The solutions are then

$$\begin{aligned} \mathfrak{z} &= \zeta\mathfrak{u}\mathrm{e}^{i\psi} + \mathrm{e}^{i(\Omega t+\Phi)}\Big(\mathfrak{r} + \mathfrak{s}\mathrm{e}^{i(\nu t+\phi)}\Big), \\ \mathfrak{z}_1 &= \zeta_1\mathfrak{u}\mathrm{e}^{i\psi} + \mathrm{e}^{i(\Omega t+\Phi)}\big(\lambda\mathfrak{r} + \lambda'\mathfrak{s}\mathrm{e}^{i(\nu t+\phi)}\big), \\ \mathfrak{z}_2 &= \zeta_2\mathfrak{u}\mathrm{e}^{i\psi} + \mathrm{e}^{i(\Omega t+\Phi)}\big(\mu\mathfrak{r} + \mu'\mathfrak{s}\mathrm{e}^{i(\nu t+\phi)}\big). \end{aligned} \tag{86}$$

Moreover, $\gamma\mathfrak{z} + \beta\mathfrak{z}_1 + \alpha\mathfrak{z}_2 = 0$ as it is the projection of $\boldsymbol{W}_0$ on a plane orthogonal to $\boldsymbol{W}_0$. This implies that the constant term $(\gamma\zeta + \beta\zeta_1 + \alpha\zeta_2)\mathfrak{u}\mathrm{e}^{i\psi}$ is also null. As $\gamma\zeta + \beta\zeta_1 + \alpha\zeta_2 = W_0$, we have necessarily $\mathfrak{u} = 0$. The solutions are thus

$$\begin{aligned}
\mathfrak{z} &= \mathrm{e}^{i(\Omega t+\Phi)}\Big(\mathfrak{r} + \mathfrak{s}\mathrm{e}^{i(\nu t+\phi)}\Big),\\
\mathfrak{z}_1 &= \mathrm{e}^{i(\Omega t+\Phi)}\Big(\lambda\mathfrak{r} + \lambda'\mathfrak{s}\mathrm{e}^{i(\nu t+\phi)}\Big),\\
\mathfrak{z}_2 &= \mathrm{e}^{i(\Omega t+\Phi)}\Big(\mu\mathfrak{r} + \mu'\mathfrak{s}\mathrm{e}^{i(\nu t+\phi)}\Big).
\end{aligned} \tag{87}$$

In this approximation, the three axes $(\mathbf{w}, \mathbf{w}_1, \mathbf{w}_2)$ describe circular motions with nutation frequency ν around the three poles $(\mathcal{P}, \mathcal{P}_1, \mathcal{P}_2)$ that precess uniformly with precession frequency Ω around the total angular momentum $\boldsymbol{W}_0$. As it was previously said, the three poles $(\mathcal{P}, \mathcal{P}_1, \mathcal{P}_2)$ remain always coplanar with $\boldsymbol{W}_0$.

4.1 Initial conditions

The preceding section shows that the solutions (87) depend only on four real numbers $\mathfrak{r}$, $\mathfrak{s}$, Φ and ϕ. At the origin of time ($t = 0$) we can choose two vectors, for instance

$$\mathfrak{z}_0 = \mathrm{e}^{i\Phi}\Big(\mathfrak{r} + \mathfrak{s}\mathrm{e}^{i\phi}\Big), \quad \text{and} \quad \mathfrak{z}_{10} = \mathrm{e}^{i\Phi}\Big(\lambda\mathfrak{r} + \lambda'\mathfrak{s}\mathrm{e}^{i\phi}\Big) \tag{88}$$

from which we derive

$$\mathfrak{r}\mathrm{e}^{i\Phi} = \frac{\lambda'\mathfrak{z}_0 - \mathfrak{z}_{10}}{\lambda' - \lambda}, \quad \text{and} \quad \mathfrak{s}\mathrm{e}^{i\phi} = \frac{\lambda\mathfrak{z}_0 - \mathfrak{z}_{10}}{\lambda - \lambda'}. \tag{89}$$

The computation of λ and λ' requires the knowledge of the averaged values $\tilde{x}$, $\tilde{y}$ and $\tilde{z}$, but it can easily be done by iteration, starting with the initial values, that is, for the first iteration

$$\tilde{x} = x(t = 0), \qquad \tilde{y} = y(t = 0), \qquad \tilde{z} = z(t = 0). \tag{90}$$

In our computations, we found that one iteration after this first try with the initial conditions was sufficient to obtain a satisfactory approximation for the frequency amplitudes and phases of the solution (see Tables 4, 7, 8).

4.2 Second order expansion

The whole previous study has been made with an Hamiltonian expanded up to the fourth degree in R/r (2), (7), (12), (13) and (14)

$$\mathcal{H} = H_T + H_E + H_I^{(0)} + H_I^{(2)} + H_I^{(4)}. \tag{91}$$

When the body-body interactions are neglected, we can restrict the analysis to the second degree in R/r. The secular Hamiltonian then simplifies to

$$\underline{H}_s = -\frac{\mathfrak{a}}{2}x^2 - \frac{\mathfrak{b}}{2}y^2 + Cte \tag{92}$$

where

$$\underline{\mathfrak{a}} = k_3 m_2 \mathcal{C}_1' \quad \text{and} \quad \underline{\mathfrak{b}} = k_3 m_1 \mathcal{C}_2' \tag{93}$$

and with

$$\begin{aligned} k_3 &= \frac{3}{2}\frac{\mathcal{G}}{a^3(1-e^2)^{3/2}} \\ \mathcal{C}_1' &= \left(1 - \frac{3}{2}\sin^2 J_1\right)\left(C_1 - \frac{A_1+B_1}{2}\right) \\ \mathcal{C}_2' &= \left(1 - \frac{3}{2}\sin^2 J_2\right)\left(C_2 - \frac{A_2+B_2}{2}\right). \end{aligned} \tag{94}$$

The secular equations (33) become

$$\begin{aligned} \dot{\mathbf{w}} &= -\frac{\underline{\mathfrak{a}}x}{\gamma}\mathbf{w}_1 \times \mathbf{w} - \frac{\underline{\mathfrak{b}}y}{\gamma}\mathbf{w}_2 \times \mathbf{w} \ , \\ \dot{\mathbf{w}}_1 &= -\frac{\underline{\mathfrak{a}}x}{\beta}\mathbf{w} \times \mathbf{w}_1 \ , \\ \dot{\mathbf{w}}_2 &= -\frac{\underline{\mathfrak{b}}y}{\alpha}\mathbf{w} \times \mathbf{w}_2 \ , \end{aligned} \tag{95}$$

where γ, β and α are still the angular momentum of the orbit, of the rotation of the primary and of the rotation of the secondary respectively. In that case, the matrix M giving the evolution of the projection of the three vectors $\mathfrak{z}$, $\mathfrak{z}_1$ and $\mathfrak{z}_2$ becomes

$$\underline{M} = \begin{pmatrix} -\frac{\underline{\mathfrak{a}}x}{\gamma}\zeta_1 - \frac{\underline{\mathfrak{b}}y}{\gamma}\zeta_2 & \frac{\underline{\mathfrak{a}}x}{\gamma}\zeta & \frac{\underline{\mathfrak{b}}y}{\gamma}\zeta \\ \frac{\underline{\mathfrak{a}}x}{\beta}\zeta_1 & -\frac{\underline{\mathfrak{a}}x}{\beta}\zeta & 0 \\ \frac{\underline{\mathfrak{b}}y}{\alpha}\zeta_2 & 0 & -\frac{\underline{\mathfrak{b}}y}{\alpha}\zeta \end{pmatrix}. \tag{96}$$

Now we use the same trick as in the equation (80), that is we replace the matrix $\underline{M}$ by the constant matrix $\underline{\tilde{M}}$

$$\underline{\tilde{M}} = \underline{M}(\tilde{x}, \tilde{y}, \tilde{z}) \tag{97}$$

where (x, y, z) have been substituted by their average. The vector ${}^t(\zeta, \zeta_1, \zeta_2)$ is still an eigenvector for the eigenvalue 0. The characteristic equation is now

$$\lambda^2 - \underline{\mathbf{T}}\lambda + \underline{\mathbf{P}} = 0 \tag{98}$$

where

$$\begin{aligned} \underline{\mathbf{T}} &= -\frac{\mathfrak{a}x}{\gamma}\zeta_1 - \frac{\mathfrak{b}y}{\gamma}\zeta_2 - \frac{\mathfrak{a}x}{\beta}\zeta - \frac{\mathfrak{b}y}{\alpha}\zeta \\ \underline{\mathbf{P}} &= \underline{\mathfrak{a}\mathfrak{b}}xy\zeta\left(\frac{\zeta}{\alpha\beta} + \frac{\zeta_1}{\gamma\alpha} + \frac{\zeta_2}{\beta\gamma}\right). \end{aligned} \tag{99}$$

These expressions give simpler formulas for the frequencies, although they still have the same form

$$\Omega = \frac{\underline{\mathbf{T}} + \sqrt{\underline{\mathbf{T}}^2 - 4\underline{\mathbf{P}}}}{2}, \qquad \nu = -\sqrt{\underline{\mathbf{T}}^2 - 4\underline{\mathbf{P}}}\ . \tag{100}$$

5 Global precession of a n-body system

We have seen that the secular motion of a two solid body system can, as in BL06, be decomposed in a uniform precession of angular motion Ω, and a periodic motion of frequency ν. In fact, this can be extended to a very general system of n solid bodies in gravitational interaction. The following result, which is of very broad application, is a consequence of the general angular momentum reduction in case of regular, quasiperiodic, motion.

Proposition 3 *Let $\mathcal{S}$ be a system of $n+1$ bodies of mass $m_i, (i = 0, \dots n)$ in gravitational interaction, with n_s solid bodies among them ($n_s \leq n+1$). Then, in a reference frame centered on one of the bodies, and for a regular quasiperiodic solution of $\mathcal{S}$, there exist a constant precession rate Ω, such that any vector $Z \in \{\mathbf{r}_i, \tilde{\mathbf{r}}_i, \boldsymbol{I}_j, \boldsymbol{J}_j, \boldsymbol{K}_j, \boldsymbol{G}_j; i = 1, \dots n; j = 1, \dots n_s\}$ has a temporal evolution that can be decomposed as*

$$Z(t) = \mathcal{R}_3(\Omega t)\tilde{Z}^{(\nu)}(t)\ , \tag{101}$$

where $\mathcal{R}_3(\Omega t)$ is a uniform precession around the total angular momentum $\boldsymbol{W}_0$ with constant rate Ω, and where $\tilde{Z}^{(\nu)}(t)$ can be expressed in term of quasiperiodic series of $3(n+n_s)-2$ frequencies (ν_k). We will call Ω the global precession rate of the system $\mathcal{S}$.

Proof. Let us consider a general system of $n+1$ bodies of mass $m_i, (i=0,\dots n)$ in gravitational interaction, with n_s solid bodies among them ($n_s \leq n+1$). This is a $3(n+1+n_s)$ degree of freedom (DOF) system. Due to the translation invariance of the system, it can be reduced to $N=3(n+n_s)$ DOF using the coordinates centered on one of the bodies (the one of mass m_0 for example). This heliocentric reduction can be made in canonical form, preserving the Hamiltonian structure of the equations (see Laskar and Robutel, 1995).

The full Hamiltonian of the system, as expressed in (1) is then a function of the vectors $(\mathbf{r}_i, \tilde{\mathbf{r}}_i, \boldsymbol{I}_j, \boldsymbol{J}_j, \boldsymbol{K}_j, \boldsymbol{G}_j), i=1,\dots n; j=1,\dots n_s$, that depends uniquely of the scalar products of theses vectors. Moreover, the total angular momentum $\boldsymbol{W}_0$ (35) is conserved.

This system, as for the usual reduction of the node, can be reduced to a system of $N-2$ degrees of freedom. A first reduction to $N-1$ DOF can be achieved by using a reference frame $(\boldsymbol{i},\boldsymbol{j},\boldsymbol{k})$ such that $\boldsymbol{k}$ is collinear with $\boldsymbol{W}_0$ and $\boldsymbol{k}\cdot\boldsymbol{W}_0$ is positive. This partial reduction is based uniquely on the fixed direction of the angular momentum (Malige et al., 2002). With this reference frame, all quasiperiodic solutions of the system can be expressed in term of only $N-1$ fundamental frequencies.

In this fixed $(\boldsymbol{i},\boldsymbol{j},\boldsymbol{k})$ reference frame, we can use canonical coordinates that are well adapted for both the orbital and rotational motions. Namely, we shall use the Andoyer coordinates for the solid bodies (L,G,H,l,g,h) (Fig. 2), and the equivalent Delaunay coordinates for the orbital motions $(\Lambda=\beta\sqrt{\mu a}, \Gamma=\Lambda\sqrt{1-e^2}, \Theta=\Gamma\cos i, M, \omega, \theta)$ where (a,e,i,M,ω,θ) are the usual elliptical elements (semi-major axis, eccentricity, inclination of the orbit with respect to the $(\boldsymbol{i},\boldsymbol{j})$ plane, mean anomaly, argument of periapse, longitude of the ascending node). For any given body of mass $m_i, i\neq 0$, $\beta_i = m_0 m_i/(m_0+m_i)$ is the reduced mass, and $\mu_i = G(m_0+m_i)$ the related gravitational constant. For any $X_i \in \{\mathbf{r}_i, \tilde{\mathbf{r}}_i; i=1,\dots n\}$, or $Y_j \in \{\boldsymbol{I}_j, \boldsymbol{J}_j, \boldsymbol{K}_j, \boldsymbol{G}_j; j=1,\dots n_s\}$, one can then write

$$\begin{aligned} X_i &= \mathcal{R}_3(\theta_i) X'_i(\Lambda_i, \Gamma_i, \Theta_i, M_i, \omega_i) \ ; \\ Y_j &= \mathcal{R}_3(h_j) Y'_j(L_j, G_j, H_j, l_j, g_j) \ . \end{aligned} \tag{102}$$

Let us now select one angle among the θ_i, h_j (θ_1 for example) and perform the usual symplectic linear change of variable

$$\begin{aligned} \theta'_1 &= \theta_1 \ ; & \Theta'_1 &= \sum_i \Theta_i + \sum_j H_j \\ \theta'_i &= \theta_i - \theta_1 \ ; & \Theta'_i &= \Theta_i \text{ for } i \neq 1 \\ h'_j &= h_j - \theta_1 \ ; & H'_j &= H_j \end{aligned} \tag{103}$$

As the Hamiltonian (1) depends only on the scalar products of X_i and Y_j, it can be as well expressed in term of scalar products of

$$\tilde{X}_i = \mathcal{R}_3(-\theta_1) X_i \ ; \qquad \tilde{Y}_j = \mathcal{R}_3(-\theta_1) Y_j \ . \tag{104}$$

Expressed in term of the new variables (103), one can see that the coordinate θ'_1 is now ignorable with an associated constant action being the modulus of the total angular momentum ($\Theta'_1 = \|\boldsymbol{W}_0\|$). The number of DOF of the system, expressed in the new coordinates $(\Lambda_i, \Gamma_i, \Theta'_i, M_i, \omega_i, \theta'_i, L_j, G_j, H'_j, l_j, g_j, h'_j)$ is now $N-2$, with one constant parameter, Θ'_1. Let us now consider a quasiperiodic solution of the above $N-2$ DOF system. All vectors $\tilde{X}_i, \tilde{Y}_j$ will be expressed in term of quasiperiodic functions on $N-2$ independent frequencies $\nu_k, (k = 1, \dots N-2)$. Finally, θ'_1 evolution is given by

$$\frac{d\theta'_1}{dt} = \frac{\partial H}{\partial \Theta'_1}(\Lambda_i, \Gamma_i, \Theta'_i, M_i, \omega_i, \theta'_{i,i\neq 1}, L_j, G_j, H'_j, l_j, g_j, h'_j) \ . \tag{105}$$

Thus $\dot{\theta}'_1(t)$ is also a quasiperiodic expression depending on the $N-2$ frequencies ν_k.

$$\frac{d\theta'_1}{dt} = \sum_{(k)} \alpha_{(k)} \exp(i < k, \nu > t) \ , \tag{106}$$

where (k) is a $(N-2)$ multi index. Let $\Omega = \alpha_{(0)}$ be the constant term of this series. We have then

$$\frac{d\theta'_1}{dt} = \Omega + \sum_{(k)\neq(0)} \alpha_{(k)} \exp(i < k, \nu > t) \ , \tag{107}$$

and thus

$$\theta_1'(t) = \Omega t + f_{(\nu)}(t) \ , \tag{108}$$

where $f_{(\nu)}(t)$ is a $(N-2)-$periodic function with frequencies (ν_k). The original vectors X_i, Y_j can then be expressed as

$$\begin{aligned} X_i &= \mathcal{R}_3(\theta_1)\tilde{X}_i = \mathcal{R}_3(\Omega t)\mathcal{R}_3(f_{(\nu)}(t))\tilde{X}_i = \mathcal{R}_3(\Omega t)\tilde{X}_i^{(\nu)} \ , \\ Y_j &= \mathcal{R}_3(\theta_1)\tilde{Y}_j = \mathcal{R}_3(\Omega t)\mathcal{R}_3(f_{(\nu)}(t))\tilde{Y}_j = \mathcal{R}_3(\Omega t)\tilde{Y}_j^{(\nu)} \ , \end{aligned} \tag{109}$$

where $\tilde{X}_i^{(\nu)}, \tilde{Y}_j^{(\nu)}$ can be expressed in term of $(N-2)-$periodic function with frequencies (ν_k). This ends the proof of the proposition.

Consequence. A consequence of this result is that for a quasiperiodic solution of the general two body problem that we are considering here $(n = 1, n_s = 2)$, the components of any vectors $\mathbf{r}, \tilde{\mathbf{r}}, \boldsymbol{I}_j, \boldsymbol{J}_j, \boldsymbol{K}_j, \boldsymbol{G}_j$, should express as quasiperiodic functions of the precessing frequency Ω and of 7 frequencies $\nu_k, k = 1, \ldots 7$, the precession frequency Ω appearing in all terms with coefficient 1. This is actually what is observed on some examples in the next section (Tables 5 and 6). One should note that the same results hold for the three body problem studied in BL06 (with $n = 2, n_s = 1$).

It is also useful to remark that the value of Ω is independent of the ν_k, i.e. any commensurable relation between Ω and the ν_k has no effect on the dynamics of the system, in the sense that it will not affect the regularity of the solutions. On the other hand, in the case of a single ν_k frequency (as for the secular system), a rational ratio Ω/ν will lead to a periodic solution in the fixed reference frame $(\boldsymbol{i}, \boldsymbol{j}, \boldsymbol{k})$. We prefer here to speak of geometric resonance instead of dynamical resonance, as there is no coupling between the two degrees of freedom of frequency Ω and ν.

6 Application

In this section we compare our rigorous results on the averaged system and our analytical approximations of the solutions of the same system with the integration of the full Hamiltonian (2), (7), (12), (13) and (14) on two different binary systems *I* and *II* (see table 1 and 2). The

physical and orbital parameters of the system *II* are those of the binary asteroid 1999 KW4 studied in FS08. We choose this system in order to compare our results with FS08. In this case, the rotation of the satellite is taken to be synchronous. As our analytical results were obtained assuming the satellite rotation asynchronous, we create a system *I* from the system *II* where the rotation of the secondary has been sped up by a factor 3. Since the orbit is circular and the initial rotation axes aligned with the axes of maximum inertia, the system *II* is highly degenerated. To get a more general system where all the fundamental frequencies will actually exist, we changed the initial Andoyer angles and the eccentricity. But then, because of its strong triaxiality, the evolution of the satellite orientation becomes chaotic (Wisdom, 1987). As here, we are concerned only with on regular behaviors, we thus decreased the satellite triaxiality and increased the semi-major axis in order to obtain a generic example of regular solution.

6.1 Numerical experiments

6.1.1 Frequency analysis

The quasiperiodic decomposition of our numerical integrations was obtained using the frequency analysis developed by Laskar (Laskar, 1988, 2005). As our systems contain a large range of frequencies going from 0.07 rad·day^{-1} to 109 rad·day^{-1}, we decided to run twice each integration with two different output time steps $h = 0.1$ days and $h' = 0.1001$ days. These two time steps do not fulfilled the Nyquist condition for the largest frequency. Nevertheless, it is possible to recover the true value ν_0 of the frequency using the following trick (Laskar, 2005). For a real x, let denote $[x]$ the real such that

$$-\pi < [x] \leq \pi. \tag{110}$$

Let ν and ν' be respectively the frequencies measured on the integration with the time step h and h'. The true frequency is given by

$$\nu_0 = \nu + \frac{[k]}{h} \tag{111}$$

where

$$k = \frac{h}{h'-h}((\nu'-\nu)h' - [\nu' h' - \nu h]). \tag{112}$$

6.1.2 System I – doubly asynchronous case

Full Hamiltonian We integrated the system I over a time span of 2 000 days and performed a frequency analysis as described above. This system contains a priori 9 degrees of freedom. Three coordinates for the orientation of each body and three coordinates for the orbit. But there is a relation between all these coordinates given by the conservation of the total angular momentum. There are thus only 8 degrees of freedom. Hence the system contains 8 fundamental frequencies (cf table 3).

These frequencies can be divided into four main categories: 1) the secular frequencies containing the precession Ω and the nutation ν; 2) the orbital frequencies with the periapse precession rate $\hat{\omega}$ and the mean motion n; 3) the frequencies of the primary $\hat{g}_1$ and $\hat{l}_1$ associated respectively to the Andoyer angles g_1 and l_1; 4) the same frequencies for the secondary $\hat{g}_2$ and $\hat{l}_2$.

Table 5 displays the frequency decomposition in the form $\sum A_j \exp i(\nu_j t + \varphi_j)$ of the motion of $\mathfrak{z}$, $\mathfrak{z}_1$ and $\mathfrak{z}_2$ (77), the projections of $\mathbf{w}$, $\mathbf{w}_1$ and $\mathbf{w}_2$ on the complex plane orthogonal to $\boldsymbol{W}_0$. The second column shows that all the frequencies are combinations of the 8 fundamental frequencies.

Moreover, we verify our proposition saying that in a frame rotating uniformly with the precession rate Ω, the system loses one degree of freedom, see section 5. Indeed, the frequency Ω appears in all the terms with the same order 1.

Averaged Hamiltonian In the frequency decomposition of the motion of $\mathbf{w}_1$ in Table 5, the nutation is only the 4^{th} term. To check the validity of the averagings, we integrated the averaged Hamiltonian (28) on the same time span (2 000 days) and we performed the same frequency analysis. Initial rotation rates, semi-major axis and eccentricity are average values computed on the numerical output of the full integration. Initial inclination, obliquities and ascending nodes were obtained from the amplitudes and the phases of the frequency analysis in

Table 5.

Table 7 displays the comparison between the frequency decomposition of the output of the averaged Hamiltonian and of the full Hamiltonian (columns 3–8). For the comparison, only the secular terms were extracted from the analysis of the full integration. The second column confirms our analytical result saying that the averaged motion contains only 2 fundamental frequencies: the precession Ω and the nutation ν; and that in a frame rotating with the precession frequency, only the nutation remains. The columns 4,5 and 7,8 show the strong agreement between the secular approach and the full integration. Even low amplitude terms such as $\Omega+2\nu$, albeit at the 57^{th} position in the decomposition of $\mathbf{w}$ in the full integration, are recovered with good amplitude and phase in the regular system.

The two last columns of table 7 give the complex amplitudes of the secular motion obtained with the analytical approximation of section 4. As in this approximation, the nutation is assumed to be a uniform rotation, there are only two terms in the description of the secular motion. Nevertheless, we see that this approximation is also in good agreement with the integration of the full Hamiltonian and of the averaged Hamiltonian.

In Table 4 are given the values of the secular frequencies for systems I and II, obtained either from the integration of the full Hamiltonian, from the integration of the averaged Hamiltonian, or with the analytical approximations (83). The precession rates are in agreement within 0.3% and the nutation frequencies within 5%.

Figure 6 represents the trajectories of the unit vectors on the plane orthogonal to the total angular momentum $\boldsymbol{W}_0$. In the left panel, the frame is fixed, it thus corresponds to $\mathcal{W}(t)$, see section 3.2. We see that the evolutions of $\mathbf{w}$ in red and $\mathbf{w}_1$ in green are dominated by the precession: their orbits are quasi-circular, whereas the orbit of $\mathbf{w}_2$ in blue contains a large nutation as it can be checked in the frequency analysis table 5. The right panel shows the same orbits but in a frame rotating with the precession rate Ω, it corresponds to $\tilde{\mathcal{W}}(t)$. It emphasizes the nutation loops. Zooms on the nutation of the orbit and of the primary are plotted on the furthest right. The solid curves are the output of the averaged Hamiltonian. The analytical approximations cannot be distinguished from the averaged output. These averaged solutions

are good approximations of the motion of $\mathbf{w}$ and $\mathbf{w}_2$ but the agreement does not seem to be as good for $\mathbf{w}_1$. Indeed, table 5 shows that high frequencies have larger amplitudes than the secular nutation.

Because of this amplitude issue for $\mathbf{w}_1$ in Fig. 6, we decided to filter our full integration with a low-pass filter to see if we could get back the averaged integration. In this scope, we reintegrated the full Hamiltonian over a time span of 20 days with an output time step of 30 min. We then filtered the output with a cutoff frequency equal to 4 rad/day. The filtered trajectories are displayed in Fig. 7. The nutation amplitude of $\mathbf{w}_1$ is now well retrieved. After a small change in the initial conditions that corresponds to a decrease of only $3.6''$ of the initial obliquity of the primary in the averaged Hamiltonian, we get back the filtered full Hamiltonian (see Fig. 8).

6.1.3 System *II* – asynchronous-synchronous case

For this second experiment, we took the same initial conditions as FS08 (table 6). The primary has an asynchronous rotation whereas the secondary rotates synchronously. The difference between our study and FS08 is that we expanded the Hamiltonian up to the fourth order in R/r where R is the radius of one body and r the distance between them. We performed the same frequency analysis as with system I. We get also 8 fundamental frequencies. Because the resonance, the frequencies associated to the secondary are not $\hat{g}_2$ and $\hat{l}_2$ anymore since they are in that case combinations of the other 6 fundamental frequencies. The two new frequencies correspond to the horizontal and vertical libration of the secondary: $\hat{\psi}_2$ and $\hat{\theta}_2$ respectively.

Table 6 presents the frequency analysis performed on this system. The result of section 5 is still valid, in a frame rotating with the precession rate, the system loses one degree of freedom. We confirm that this result does not depend on the resonances in the reduced problem.

The averaged Hamiltonian and the analytical approximation were not specifically written for such a resonant case. Regardless of this fact, the results of the averaged Hamiltonian and of the analytical approximation applied to this system are summarized in table 8. It is remarkable that the first two amplitudes of each vector are in good agreement with the full integration.

Nevertheless, the third amplitude of $\mathbf{w}_2$ is wrong by a factor 3. The values of these secular frequencies are given at the bottom of table 4. The use of the averaged Hamiltonian or of the analytical approximations leads to an error on the precession rate equal to 1% and on the nutation rate equal to 24%.

6.2 Comparison with FS08

6.2.1 Numerical results

In FS08, Fahnestock and Scheeres expanded the Hamiltonian up to the second order in R/r. They find that motions of binary asteroids such as 1999 KW4 are combinations of four modes with their respective fundamental frequency. The first and fastest mode corresponds to the rotation of the primary around its axis. The second mode coincides with the orbital motion which has the same period as the rotation of the secondary around its axis. The third mode is said to be an excitation of the satellite's free precession dynamics and has a period of ≈ 188 h. The corresponding frequency would be ≈ 0.802 rad/day. The last mode is identified as the precession motion.

Our results generally agree with the analysis of Fahnestock and Scheeres. Nevertheless, several frequencies are missing in their analysis, probably because of the degeneracy of their initial conditions. As the initial eccentricity is close to 0, and the angular momenta along the axes of maximum inertia, the first terms in the frequency decompositions are combinations of $\hat{\omega} + n$ which corresponds to their orbital frequency, and of $\hat{g}_1 + \hat{l}_1$ which corresponds to their rotation of the primary, see table 6. On the other hand, we do not find their third mode of frequency ≈ 0.802 rad/day.

6.2.2 Solid-point interaction

Fahnestock and Scheeres found also that the spin axis of the primary and the orbital plane precess at the same rate. They derived an analytical expression for this precession rate, see their equation (76). Their result corresponds in fact to the solution of the single planet case that is

already described in BL06 and which does not require the more elaborated formalism developed here. Indeed, as they expanded the potential up to the second order only, they canceled the effect of the orientation of the secondary on the precession of the primary ($\mathfrak{c} = \mathfrak{d} = \mathfrak{e} = \mathfrak{f} = \mathfrak{g} = 0$). Moreover, as they fixed the orientation of the secondary with the orbit, the secondary does not influence the orbit ($y = (\mathbf{w}\cdot\mathbf{w}_2) = 1$). We recall here the derivation of this frequency as given in BL06. With the assumption of a point mass satellite, the Hamiltonian becomes

$$\mathcal{H} = -\frac{\mathfrak{a}}{2}x^2, \tag{113}$$

with $x = (\mathbf{w}\cdot\mathbf{w}_1)$ and

$$\begin{aligned}\dot{\mathbf{w}} &= -\frac{\mathfrak{a}}{\gamma}(\mathbf{w}\cdot\mathbf{w}_1)\mathbf{w}_1\times\mathbf{w},\\ \dot{\mathbf{w}_1} &= -\frac{\mathfrak{a}}{\beta}(\mathbf{w}\cdot\mathbf{w}_1)\mathbf{w}\times\mathbf{w}_1.\end{aligned} \tag{114}$$

This reduced problem has 5 independent integrals given by

$$\begin{aligned}&\|\mathbf{w}\| = 1\\ &\|\mathbf{w}_1\| = 1\\ &\gamma\mathbf{w} + \beta\mathbf{w}_1 = \boldsymbol{W}_0\ .\end{aligned} \tag{115}$$

As $x = \mathbf{w}\cdot\mathbf{w}_1$ is constant, the system is trivially integrable. We have indeed

$$\dot{\mathbf{w}} = \Omega_0\mathbf{w}_0\times\mathbf{w}\ , \quad \dot{\mathbf{w}}_1 = \Omega_0\mathbf{w}_0\times\mathbf{w}_1\ ; \tag{116}$$

where $\mathbf{w}_0 = \boldsymbol{W}_0/\left\|\boldsymbol{W}_0\right\|$ is the unit vector in the direction of the total angular momentum $\boldsymbol{W}_0$, and

$$\Omega_0 = -\frac{\mathfrak{a}x}{\gamma}\sqrt{1 + \frac{\gamma^2}{\beta^2} + 2\frac{\gamma}{\beta}x}\ . \tag{117}$$

Both vectors $\mathbf{w}, \mathbf{w}_1$ thus precess uniformly around the total angular momentum direction $\mathbf{w}_0$ with constant precession rate Ω_0. The correspondence with the notations of the equation

(76) of FS08 is

$$\begin{aligned} \frac{\mathfrak{a}}{\gamma} &= \frac{3}{2}\frac{\sqrt{\mu}}{a^{7/2}(1-e^2)^2}(I_1 - I_{\rm eq})\left(1 - \frac{3}{2}\sin^2 J_1\right) \\ x &= \cos(\delta + i) \\ \sqrt{1 + \frac{\gamma^2}{\beta^2} + 2\frac{\gamma}{\beta}x} &= \frac{\sin(\delta+i)}{\sin i}. \end{aligned} \tag{118}$$

Remark. The factor $(1 - (3/2)\sin^2 J_1)$ is not in FS08 because FS08 assumes that the primary angular momentum is aligned with its figure axis ($J_1 = 0$). This is not the case in this paper where we do not require this simplification.

7 Conclusions

We have shown here that the general framework developed in BL06 applies as well to the problem of two rigid bodies orbiting each other. This formalism enables us to obtain the long term evolution of the spin axis of the two bodies as well as the evolution of the orientation of the orbital plane. The two bodies can be very general, with strong triaxiality, and their rotation vector is not necessary aligned with their axis of maximum inertia. The gravitational potential is expanded up to the fourth order so as to keep the direct interaction between the orientation of the two bodies, and as in BL06, the evolution of their spin axis is obtained after a suitable averaging.

We found that the secular evolution is composed of two periodic motions: a global precession of the three angular momenta and nutation loops. As in BL06, the nutation loops are symmetric with respect to a plane containing the total angular momentum and precessing with the global precession frequency. We gave analytical approximations of these frequencies.

We performed a frequency analysis (Laskar, 1988, 2005) on a numerical integration of the full Hamiltonian. We chose the typical binary asteroid system 1999 KW4 already analyzed in FS08. We retrieved the precession and the nutation motions predicted by the secular Hamiltonian and estimated by the analytical approximations. On a non resonant system, derived from 1999 KW4, the secular solution, and the analytical results agree extremely well with the full solution.

This is still the case to a lesser extent with the more specific case of 1999 KW4, which is in 1:1 spin-orbit resonance. In a further work, we could consider in a more precise way the possible resonances. In that case, some of the averagings need to be done in a different way, probably leading to less symmetrical, more complex, expressions. The main goal reached by the present paper was to search, in this apparently difficult problem of two solid bodies in interaction, what was the most simple relevant underlying structure. One can now add possible additional effects, as tidal dissipation, and still consider the problem with the present setting. We thus expect that the results presented here will be helpful for the understanding of the general evolution of binary asteroids, or other problems of astronomical interest.

In the elaboration of this paper, we came across the very general result given in our proposition 3 which applies to any system of n massive bodies (point masses or not) in gravitational interaction. This property of the motion states that the general regular quasiperiodic motions with N independent frequencies can be decomposed into a uniform rotation around the total angular momentum, which we call the global precession, and in this rotation frame, a quasiperiodic motion with $N-1$ frequencies, independent of the global precession frequency.

Acknowledgments

We thank Franck Marchis for discussions on binary asteroids observations. The authors largely benefitted from the interactions and discussions inside the Astronomy and Dynamical System group at IMCCE.

Appendix A. Gravitational interaction expansion

The gravitational interaction between the two bodies is given by (5)

$$H_I = -\iint \frac{\mathcal{G}\, dm_1\, dm_2}{\|\mathbf{r} + \mathbf{r}_2 - \mathbf{r}_1\|} \,. \tag{119}$$

The expansion of this potential in Legendre polynomials leads to the following integrals

$$
\begin{aligned}
H_I^{(0)} &= -\frac{\mathcal{G}}{r}\iint \quad dm_1\, dm_2 \ , \\
H_I^{(1)} &= 0 \\
H_I^{(2)} &= -\frac{\mathcal{G}}{2r^3}\iint \left[3(\mathbf{u}\cdot\mathbf{r}_1)^2 + 3(\mathbf{u}\cdot\mathbf{r}_2)^2 - r_1^2 - r_2^2\right] dm_1\, dm_2 \\
H_I^{(3)} &= -\frac{\mathcal{G}}{2r^4}\iint \Big[5(\mathbf{u}\cdot\mathbf{r}_1)^3 - 5(\mathbf{u}\cdot\mathbf{r}_2)^3 \\
&\qquad\qquad -3r_1^2(\mathbf{u}\cdot\mathbf{r}_1) + 3r_2^2(\mathbf{u}\cdot\mathbf{r}_2)\Big]\, dm_1\, dm_2 \\
H_I^{(4)} &= -\frac{\mathcal{G}}{8r^5}\iint \Big[35(\mathbf{u}\cdot\mathbf{r}_1)^4 + 35(\mathbf{u}\cdot\mathbf{r}_2)^4 \\
&\qquad\qquad -120(\mathbf{r}_1\cdot\mathbf{r}_2)(\mathbf{u}\cdot\mathbf{r}_1)(\mathbf{u}\cdot\mathbf{r}_2) \\
&\qquad\qquad -12\mathbf{r}_1^2(\mathbf{r}_1\cdot\mathbf{r}_2) + 210(\mathbf{u}\cdot\mathbf{r}_2)^2(\mathbf{u}\cdot\mathbf{r}_1)^2 \\
&\qquad\qquad -30\mathbf{r}_2^2(\mathbf{u}\cdot\mathbf{r}_1)^2 - 30r_1^2(\mathbf{u}\cdot\mathbf{r}_2)^2 \\
&\qquad\qquad -30r_1^2(\mathbf{u}\cdot\mathbf{r}_1)^2 - 30r_2^2(\mathbf{u}\cdot\mathbf{r}_2)^2 \\
&\qquad\qquad +3r_2^4 + 3r_1^4 + 6r_1^2r_2^2\Big]\, dm_1\, dm_2
\end{aligned}
\tag{120}
$$

where all linear terms in $\mathbf{r}_1$ or $\mathbf{r}_2$ have been omitted since these two vectors are expressed relative to the barycenter of the respective body and their integral vanishes. In the section 2.3, an additional hypothesis is made on the mass distribution of each body that simplifies the potential. They are supposed to be symmetrical relative to the planes perpendicular to the principal axes of inertia. As a consequence, the integral of any odd power of $\mathbf{r}_1$ or $\mathbf{r}_2$ cancels.

Appendix B. Inertia integral

Inertia integrals of homogeneous ellipsoids are computed in the following way. Let a, b, c be the three semi-axes of a homogeneous ellipsoid $\mathcal{E}$ of density ρ. The total mass of the ellipsoid is

$$m = \frac{4\pi}{3}\rho abc \tag{121}$$

and the second order inertia integrals are

$$\begin{aligned}
\int_{\mathcal{E}} \rho x^2 \, dx \, dy \, dz &= \rho a^3 bc \int_{\mathcal{B}} X^2 \, dX \, dY \, dZ = \frac{1}{5} m a^2 \ , \\
\int_{\mathcal{E}} \rho y^2 \, dx \, dy \, dz &= \rho a b^3 c \int_{\mathcal{B}} Y^2 \, dX \, dY \, dZ = \frac{1}{5} m b^2 \ , \\
\int_{\mathcal{E}} \rho z^2 \, dx \, dy \, dz &= \rho a b c^3 \int_{\mathcal{B}} Z^2 \, dX \, dY \, dZ = \frac{1}{5} m c^2 \ ,
\end{aligned} \tag{122}$$

where $X = x/a$, $Y = y/b$, $Z = z/c$ and $\mathcal{B}$ is the unit ball. From the definition of the moments of inertia

$$\begin{aligned}
A &= \int_{\mathcal{E}} (y^2 + z^2) \, dm \ , \\
B &= \int_{\mathcal{E}} (z^2 + x^2) \, dm \ , \\
C &= \int_{\mathcal{E}} (x^2 + y^2) \, dm \ ,
\end{aligned} \tag{123}$$

we get relations between the semi-axes and the moments of inertia

$$\begin{aligned}
a^2 &= \frac{5}{2m}(-A + B + C) \ , \\
b^2 &= \frac{5}{2m}(A - B + C) \ , \\
c^2 &= \frac{5}{2m}(A + B - C) \ .
\end{aligned} \tag{124}$$

General expressions of the inertia integrals are thus

$$\int_{\mathcal{E}} x^i y^j z^k \, dm = \frac{3}{4\pi} m a^i b^j c^k \int_{\mathcal{B}} X^i Y^j Z^k \, dX \, dY \, dZ \ , \tag{125}$$

with a, b, c given by (124).

Appendix C. Averaged quantities

In this appendix, we give general formulas for the averaging over the orbital mean motions. The integrals will be computed using the true anomaly (ν) as an intermediate variable. We recall

first the basic formulas

$$\begin{aligned} dM &= \frac{r^2}{a^2\sqrt{1-e^2}}d\nu \\ \mathcal{X} &= r\cos\nu \\ \mathcal{Y} &= r\sin\nu \\ r &= \frac{a(1-e^2)}{1+e\cos\nu} \end{aligned} \tag{126}$$

where $\mathcal{X}$ and $\mathcal{Y}$ are the coordinates of a point on a keplerian orbit in the reference frame $(\boldsymbol{i}, \boldsymbol{j}, \boldsymbol{k})$ with $\boldsymbol{i}$ and $\boldsymbol{k}$ respectively in the direction of periapse and angular momentum.

Intermediate integrals

In the following, we handle integrals such as Wallis integrals. We recall their expression. Let

$$I_n = \frac{1}{2\pi}\int_0^{2\pi} \cos^n t\, dt = \frac{1}{2\pi}\int_0^{2\pi} \sin^n t\, dt \tag{127}$$

and

$$\begin{aligned} J_{n,m} &= \frac{1}{2\pi}\int_0^{2\pi} \sin^m t \cos^n t\, dt \\ &= \frac{1}{2\pi}\int_0^{2\pi} \sin^n t \cos^m t\, dt. \end{aligned} \tag{128}$$

We have then

$$I_n = \begin{cases} 0 & \text{if } n \text{ is odd,} \\ \dfrac{(2p)!}{2^{2p}(p!)^2} & \text{if } n = 2p,\ p \in \mathbb{N}\ , \end{cases} \tag{129}$$

and for $p \geq 0$, $I_{2(p+1)}$ can be computed using the recurrence formula

$$I_{2(p+1)} = \frac{2p+1}{2p+2} I_{2p}. \tag{130}$$

The integrals $J_{n,m}$ are null whenever n or m is odd, else their values are a sum of integrals I_k

$$\begin{aligned} J_{2p,2q} &= \frac{1}{2\pi}\int_0^{2\pi} (1-\cos^2 t)^p \cos^{2q} t\, dt, \\ &= \sum_{k=0}^{p} (-1)^k \binom{p}{k} I_{2q+2k} \\ &= \sum_{k=0}^{q} (-1)^k \binom{q}{k} I_{2p+2k}. \end{aligned} \tag{131}$$

The last equality comes from $J_{n,m} = J_{m,n}$.

Computation of $\langle 1/r^n \rangle$ for $n \geq 2$

From these results, we can write

$$\begin{aligned}\left\langle \frac{1}{r^n} \right\rangle &= \frac{1}{a^n(1-e^2)^{n-3/2}} \frac{1}{2\pi} \int_0^{2\pi} (1+e\cos\nu)^{n-2}\, d\nu, \\ &= \frac{1}{a^n(1-e^2)^{n-3/2}} \sum_{p=0}^{\mathrm{E}(n/2-1)} \binom{n-2}{2p} I_{2p} e^{2p}, \\ &= \frac{1}{a^n(1-e^2)^{n-3/2}} \sum_{p=0}^{\mathrm{E}(n/2-1)} \mathcal{A}_n(p) e^{2p},\end{aligned} \tag{132}$$

where $\mathrm{E}(x)$ returns the integer part of x and

$$\mathcal{A}_n(p) = \binom{n-2}{2p} \frac{(2p)!}{2^{2p}(p!)^2}. \tag{133}$$

The recurrence relation for $\mathcal{A}_n(p)$ is

$$\mathcal{A}_n(p+1) = \frac{(n-2p-2)(n-2p-3)}{(2p+2)^2} \mathcal{A}_n(p) \tag{134}$$

with $\mathcal{A}_n(0) = 1$.

Computation of $\left\langle \mathcal{X}^m \mathcal{Y}^n / r^l \right\rangle$ for $l \geq m+n+2$

In averaging computations we meet integrals in the form

$$\left\langle \frac{(\mathbf{r}\cdot\boldsymbol{s}_1)^{k_1} \cdots (\mathbf{r}\cdot\boldsymbol{s}_j)^{k_j}}{r^l} \right\rangle . \tag{135}$$

These integrals can be computed from

$$\begin{aligned}\left\langle \frac{\mathcal{X}^m \mathcal{Y}^n}{r^l} \right\rangle &= \frac{1}{a^h(1-e^2)^{h-3/2}} \frac{1}{2\pi} \\ &\quad \times \int_0^{2\pi} \cos^m\nu \sin^n\nu (1+e\cos\nu)^{h-2}\, d\nu, \\ &= \frac{1}{a^h(1-e^2)^{h-3/2}} \sum_{k=0}^{h-2} \binom{h-2}{2k} J_{n,m+k} e^k,\end{aligned} \tag{136}$$

where $h = l-m-n$ and $J_{n,m}$ defined as previously. This integral is null whenever n is odd.

References

Abul'naga, M.Z., Barkin, I.V., 1979. Regular motions of a body in the gravity field of a sphere. Astron. Zh. 56, 881-887.

Andoyer, H., 1923. Cours de Mécanique Céleste, vol. 1. Gauthier-Villars, Paris.

Ashenberg, J., 2007. Mutual gravitational potential and torque of solid bodies via inertia integrals. Celest. Mech. 99, 149–159.

Borderies, N., 1978. Mutual gravitational potential of N solid bodies. Celest. Mech. 18, 295–307.

Borisov, A.V., Mamaev, I.S., 2005. Dynamics of the Rigid Body. R&C Dynamics, Moscow *(in russian)*.

Boué, G., Laskar, J., 2006. Precession of a planet with a satellite. Icarus 185, 312–330.

Boué, G., Laskar, J., 2008. Erratum: Precession of planet with a satellite. hal.archives-ouvertes.fr:hal-00335321_v2.

Colombo, G., 1966. Cassini's second and third laws. Astron. J. 71, 891–896.

Duboshin, G.N., 1958. The Differential Equations of Translational - Rotational Motion of Mutually Attracting Rigid Bodies. Soviet Astronomy 2, 239-+.

Fahnestock, E.G., Scheeres, D.J., 2008. Simulation and analysis of the dynamics of binary near-Earth Asteroid (66391) 1999 KW4. Icarus 194, 410–435.

Hénon, M., 1983. in Chaotic Behavior of Deterministic Systems. edited by Ioos, G., Hellman, R. G. H., and Stora, R. (North-Holland, Amsterdam, 1983).

Laskar, J., 1988. Secular evolution of the solar system over 10 million years. Astron. Astrophys. 198, 341–362.

Laskar, J., 2005. Frequency Map analysis and quasi periodic decompositions. in Hamiltonian systems and Fourier analysis, Benest et al., eds, Cambridge Scientific Publishers, Cambridge.

Laskar, J., Robutel, P., 1995. Stability of the Planetary Three-Body Problem. I. Expansion of the Planetary Hamiltonian. Celest. Mech. 62, 193–217.

Maciejewski, A.J., 1995. Reduction, Relative Equilibria and Potential in the Two Rigid Bodies Problem. Celest. Mech. 63, 1–28.

Malige, F., Robutel, P., Laskar, J., 2002. Partial Reduction in the N-body Planetary Problem using the Angular Momentum Integral. Celest. Mech. 84, 283–316.

Paul, M.K., 1988. An Expansion in Power Series of Mutual Potential for Gravitating Bodies with Finite Sizes. Celest. Mech. 44, 49–59.

Peale, S.J., 1969. Generalized Cassini's Laws. Astron. J. 74, 483–489.

Tricarico, P., 2008. Figure-figure interaction between bodies having arbitrary shapes and mass distributions: a power series expansion approach. Celest. Mech. 100, 319–330.

Wang, L.-S., Krishnaprased, P.S., Maddocks, J.H., 1991. Hamiltonian dynamics of a rigid body in a central gravitational field. Celest. Mech. 50, 349–386.

Ward, W.R., 1975. Tidal friction and generalized Cassini's laws in the solar system. Astron. J. 80, 64–70.

Wisdom, J., Peale, S.J., Mignard, F., 1984. The Chaotic Rotation of Hyperion. Icarus 58, 137–152.

Wisdom, J., 1987. Rotational dynamics of irregularly shaped natural satellites. Astron. J. 94, 1350–1360.

Tables and Figures

Table 1: Physical and orbital parameters of a fictitious doubly asynchronous binary system. m is the mass, A, B and C are the moments of inertia divided the mass, w is the rotation rate, h, I, g, J and l are the Andoyer angles of the two solid bodies as defined in Fig. 2.

System I

	Primary	Secondary		Orbit
m (10^{12}kg)	2.5	0.15	a (km)	2.75
A (km^2)	0.17	0.0165	λ (deg)	0.0
B (km^2)	0.18	0.017	e	0.035
C (km^2)	0.19	0.025	ω (deg)	0.0
w ($^\circ$/day)	3125.34	1500	i (deg)	0.0
h (deg)	100.82	-110.0	Ω (deg)	0.0
I (deg)	10.74	5.0		
g (deg)	112.03	-180.0		
J (deg)	3.0	5.0		
l (deg)	90.0	90.0		

Table 2: Physical and orbital parameters of the binary asteroids 1999 KW4 given by FS08. m is the mass, A, B and C are the moments of inertia divided the mass, w is the rotation rate, h, I, g, J and l are the Andoyer angles of the two solid bodies as defined in Fig. 2.

System *II*

	Primary	Secondary		Orbit
m (10^{12}kg)	2.353	0.135	a (km)	2.5405
A (km^2)	0.1648	0.01608	λ (deg)	0.0
B (km^2)	0.1726	0.02374	e	0.0
C (km^2)	0.1959	0.02799	ω (deg)	0.0
w ($^\circ$/day)	3125.34	498.09	i (deg)	0.0
h (deg)	117.04	0.0	Ω (deg)	0.0
I (deg)	10.0	0.0		
g (deg)	0.0	0.0		
J (deg)	0.0	0.0		
l (deg)	-173.93	180.0		

Table 3: Fundamental frequencies of the two systems. Ω and ν are the precession and nutation frequencies respectively. ω and n correspond to the precession of the periastre and the mean motion. $\hat{g}_1$ and $\hat{l}_1$ on the one hand, and $\hat{g}_2$ and $\hat{l}_2$ on the other hand, are associated to the Andoyer angles. $\hat{\psi}_2$ and $\hat{\theta}_2$ are the horizontal and vertical libration frequencies in the resonant system *II*.

frequency	value (rad/day)	
	system *I*	system *II*
Ω	-0.0312	-0.0713
ν	-0.9788	-4.7488
$\hat{\omega}$	0.0681	-0.0902
n	8.0052	9.0503
$\hat{g}_1$	58.9763	63.3416
$\hat{l}_1$	-4.4062	-8.7218
$\hat{g}_2$	39.9703	–
$\hat{l}_2$	-13.9042	–
$\hat{\psi}_2$	–	7.5914
$\hat{\theta}_2$	–	4.1475

Table 4: Secular frequencies. Comparison between the integration of the full Hamiltonian, the integration of the averaged Hamiltonian and the analytical approximations.

		Ω	ν
system	type	(rad/day)	(rad/day)
	full	-0.0312	-0.9788
syst. *I*	averaged	-0.0310	-1.1276
	calculation	-0.0310	-1.1091
	full	-0.0713	-4.7488
syst. *II*	averaged	-0.0710	-3.5982
	calculation	-0.0710	-3.5629

Table 5: Frequency decomposition of the motion of the projections $\mathfrak{z}$, $\mathfrak{z}_1$ and $\mathfrak{z}_2$ respectively of $\mathbf{w}$, $\mathbf{w}_1$ and $\mathbf{w}_2$ on the plane orthogonal to the total angular momentum $\boldsymbol{W}_0$. The integration was made using the full Hamiltonian with the initial conditions of the doubly asynchronous system I. Only the first 20 terms of the series $\sum A_j \exp i(\nu_j t + \varphi_j)$ are displayed for each vector. In order to simplify the reading, hats on the angles ω, g_1, l_1, g_2 and l_2 are omitted.

var.	i		ν_i (rad.yr^{-1})	$A_i^{(f)}$ ($''$)	$\varphi_i^{(f)}$ (deg)
	1	Ω	-0.0312	29105.09	-169.37
	2	$\Omega+\nu$	-1.0100	209.11	-17.70
	3	$\Omega+2\omega+2n$	16.1156	55.87	-10.55
	4	$\Omega-\nu+2\omega+2n$	17.0943	12.29	-162.22
	5	$\Omega+2\omega+2n-g_2$	-23.8548	9.55	-158.86
	6	$\Omega+2\omega+2n-g_1$	-42.8607	6.70	57.27
	7	$\Omega+g_2$	39.9391	5.72	-21.06
	8	$\Omega-n$	-8.0365	5.22	-168.69
	9	$\Omega+n$	7.9740	5.21	9.94
$\mathbf{w}$	10	$\Omega+g_1$	58.9451	4.89	122.82
	11	$\Omega+2\omega+3n$	24.1208	4.00	-11.23
	12	$\Omega+2\omega+2n-2l_1-2g_1$	-93.0245	3.39	-55.00
	13	$\Omega+2l_1+2g_1$	109.1089	2.90	-124.92
	14	$\Omega+2\omega+n$	8.1103	1.70	170.13
	15	$\Omega+2\omega+3n-g_2$	-15.8495	1.47	-159.55
	16	$\Omega+2\omega+2n-2l_1-g_1$	-34.0483	1.39	57.17
	17	$\Omega+\nu+n$	6.9953	1.08	161.62
	18	$\Omega+\nu-n$	-9.0152	1.04	-17.02
	19	$\Omega-\nu$	0.9476	0.95	-141.05
	20	$\Omega+2l_1+g_1$	50.1326	0.94	122.90
	1	Ω	-0.0312	9687.25	10.63
	2	$\Omega+2\omega+2n$	16.1156	18.80	169.45
	3	$\Omega+2\omega+2n-g_1$	-42.8607	2.26	-122.72
	4	$\Omega+\nu$	-1.0100	1.86	162.30
	5	$\Omega-n$	-8.0365	1.73	11.31
	6	$\Omega+n$	7.9740	1.73	-170.06
	7	$\Omega+g_1$	58.9451	1.60	-57.20
	8	$\Omega+2\omega+3n$	24.1208	1.34	168.77
	9	$\Omega-2\omega-2n+2l_1+2g_1$	92.9621	1.11	76.25
$\mathbf{w}_1$	10	$\Omega+2l_1+2g_1$	109.1089	0.94	55.08
	11	$\Omega+2\omega+n$	8.1103	0.58	-9.87
	12	$\Omega+2\omega+2n-2l_1-g_1$	-34.0483	0.47	-122.83
	13	$\Omega+2l_1+g_1$	50.1326	0.31	-57.10
	14	$\Omega+2\omega+3n-g_1$	-34.8555	0.30	-123.41
	15	$\Omega-2\omega-2n$	-16.1780	0.16	-148.19
	16	$\Omega-2\omega-3n+2l_1+2g_1$	84.9569	0.13	76.94
	17	$\Omega-\nu+2\omega+2n$	17.0943	0.13	17.78
	18	$\Omega-n+g_1$	50.9398	0.08	-56.52
	19	$\Omega+2\omega+4n$	32.1260	0.07	168.08
	20	$\Omega+2\omega+3n-2l_1-g_1$	-26.0430	0.07	-123.51
	1	Ω	-0.0312	30079.18	-169.37
	2	$\Omega+\nu$	-1.0100	17781.88	162.30
	3	$\Omega-\nu+2\omega+2n$	17.0943	1040.78	17.78
	4	$\Omega+2\omega+2n-g_2$	-23.8548	829.13	21.13
	5	$\Omega+g_2$	39.9391	495.19	158.94
	6	$\Omega+2\omega+3n-g_2$	-15.8495	126.95	20.45
	7	$\Omega-\nu$	0.9476	96.54	38.96
	8	$\Omega+\nu+n$	6.9953	90.98	-18.39
	9	$\Omega+\nu-n$	-9.0152	87.74	162.98
$\mathbf{w}_2$	10	$\Omega-\nu+2\omega+3n$	25.0996	74.38	17.10
	11	$\Omega-\nu+2\omega+n$	9.0891	50.41	-161.54
	12	$\Omega+2\omega+2n$	16.1156	46.84	-10.55
	13	$\Omega-n+g_2$	31.9339	25.33	159.63
	14	$\Omega+2\omega+2n-2l_2-g_2$	3.9537	23.66	-161.23
	15	$\Omega+n+g_2$	47.9444	21.72	158.26
	16	$\Omega+2\omega+4n-g_2$	-7.8443	19.43	19.77
	17	$\Omega+2n+2l_1-2l_2$	34.9754	14.90	-57.53
	18	$\Omega-\nu+2l_2+2g_2$	53.0797	10.87	-22.05
	19	$\Omega+2l_2+g_2$	12.1306	8.74	161.31
	20	$\Omega+2\omega+5n-g_2$	0.1610	7.16	-160.92

Table 6: Same as table 5 for the system *II*.

var.	i		ν_i (rad.yr^{-1})	$A_i^{(f)}$ ($''$)	$\varphi_i^{(f)}$ (deg)
	1	Ω	-0.0713	27979.553	-153.15
	2	$\Omega + 2\omega + 2n$	17.8490	111.214	-26.81
	3	$\Omega + \nu$	-4.8201	4.421	-160.28
	4	$\Omega + 2\omega + 2n - 2l_1 - 2g_1$	-91.3906	3.320	-39.33
	5	$\Omega - n$	-9.1216	2.847	25.69
	6	$\Omega + 2l_1 + 2g_1$	109.1682	2.779	-140.63
	7	$\Omega + n$	8.9790	2.678	-151.99
	8	$\Omega + 2\omega + 3n$	26.8993	2.201	154.37
	9	$\Omega + \psi_2$	7.5201	1.295	-152.20
$\mathbf{w}$	10	$\Omega - \psi_2$	-7.6627	1.117	25.96
	11	$\Omega + 2\omega + n$	8.7986	1.066	-27.97
	12	$\Omega - \nu + 2\omega + 2n$	22.5978	0.942	-19.67
	13	$\Omega + 2\omega + 2n + \psi_2$	25.4404	0.828	155.16
	14	$\Omega - 2\omega - 2n$	-17.9916	0.490	-99.49
	15	$\Omega + \omega + n - \theta_2$	4.7413	0.376	-163.33
	16	$\Omega + 2\omega + 2n - \psi_2$	10.2575	0.280	-27.75
	17	$\Omega + \omega - \theta_2$	-4.3090	0.237	-164.49
	18	$\Omega - \nu + 2\omega - n$	-4.5532	0.170	156.75
	19	$\Omega - \nu + 2\omega$	4.4971	0.161	157.74
	20	$\Omega + \nu + n$	4.2302	0.143	20.77
	1	Ω	-0.0713	8008.982	26.85
	2	$\Omega + 2\omega + 2n$	17.8490	32.172	153.19
	3	$\Omega - 2\omega - 2n + 2l_1 + 2g_1$	91.2480	0.939	93.03
	4	$\Omega - n$	-9.1216	0.796	-154.31
	5	$\Omega + n$	8.9790	0.794	28.01
	6	$\Omega + 2l_1 + 2g_1$	109.1682	0.780	39.37
	7	$\Omega + 2\omega + 3n$	26.8993	0.636	-25.64
	8	$\Omega - \psi_2$	-7.6627	0.325	-154.10
	9	$\Omega + \psi_2$	7.5201	0.324	27.80
$\mathbf{w}_1$	10	$\Omega + 2\omega + n$	8.7986	0.301	152.03
	11	$\Omega - 2\omega - 2n$	-17.9916	0.243	-99.49
	12	$\Omega + 2\omega + 2n + \psi_2$	25.4404	0.232	-25.86
	13	$\Omega + 2\omega + 2n - \psi_2$	10.2575	0.093	152.25
	14	$\Omega - 2\omega - 3n + 2l_1 + 2g_1$	82.1976	0.031	-88.11
	15	$\Omega + \nu$	-4.8201	0.030	19.72
	16	$\Omega + 4\omega + 4n - 2l_1 - 2g_1$	-73.4703	0.029	87.00
	17	$\Omega + 2\omega$	-0.2517	0.024	-29.13
	18	$\Omega + 2\omega + 2n - 2l_1 - 2g_1$	-91.3906	0.023	140.67
	19	$\Omega + n - \psi_2$	1.3876	0.020	-152.96
	20	$\Omega - n + \psi_2$	-1.5302	0.020	26.63
	1	Ω	-0.0713	28848.685	-153.15
	2	$\Omega + \nu$	-4.8201	924.226	19.72
	3	$\Omega - \nu + 2\omega + 2n$	22.5978	196.275	160.33
	4	$\Omega + 2\omega + 2n$	17.8490	81.967	-26.85
	5	$\Omega + \omega + n - \theta_2$	4.7413	77.510	16.67
	6	$\Omega + \nu + n$	4.2302	55.301	-159.15
	7	$\Omega + \omega - \theta_2$	-4.3090	47.469	15.51
	8	$\Omega - \nu + 2\omega - n$	-4.5532	34.386	-23.16
	9	$\Omega - \nu + 2\omega$	4.4971	33.518	-22.15
$\mathbf{w}_2$	10	$\Omega + \nu - \psi_2$	-12.4116	30.128	18.77
	11	$\Omega + \omega + n + \theta_2$	13.0363	29.773	-16.63
	12	$\Omega - \psi_2$	-7.6627	29.524	-151.52
	13	$\Omega + \omega + \theta_2$	3.9860	26.699	162.21
	14	$\Omega + \nu - n$	-13.8705	26.395	-161.45
	15	$\Omega + \omega - n + \theta_2$	-5.0643	19.869	-18.95
	16	$\Omega + \nu + \psi_2$	2.7713	19.196	20.64
	17	$\Omega + \omega + n - \psi_2 + \theta_2$	5.4449	18.432	162.43
	18	$\Omega + \nu + 2n$	13.2805	13.450	22.33
	19	$\Omega - \nu + 2\omega + 2n - \psi_2$	15.0063	12.645	159.39
	20	$\Omega + \omega + n - \psi_2 - \theta_2$	-2.8501	12.132	-164.27

Table 7: Frequency analysis of the doubly asynchronous system I. Columns 3 to 5 correspond to the frequency analysis performed on the numerical integration of the averaged hamiltonian (28), superscript (a). Columns 6 to 8 contain the secular terms of the frequency decompositions computed on the output of the full integration, superscript (f). Columns 9 to 11 are the results of the analytical approximations (83 and 89), superscript (c).

var.		i	$A_i^{(a)}$ ($''$)	$\varphi_i^{(a)}$ (deg)	i	$A_i^{(f)}$ ($''$)	$\varphi_i^{(f)}$ (deg)	i	$A_i^{(c)}$ ($''$)	$\varphi_i^{(c)}$ (deg)
$\mathbf{w}$	Ω	1	29104.12	-169.37	1	29105.09	-169.37	1	29108.16	-169.37
	$\Omega+\nu$	2	209.34	-17.37	2	209.11	-17.70	2	212.43	-17.10
	$\Omega-\nu$	3	0.95	-141.38	19	0.95	-141.05			
	$\Omega+2\nu$	4	0.04	134.64	57	0.04	134.09			
$\mathbf{w}_1$	Ω	1	9688.12	10.63	1	9687.25	10.63	1	9688.16	10.63
	$\Omega+\nu$	2	1.76	162.63	4	1.86	162.30	2	1.85	162.90
	$\Omega-\nu$	3	0.05	-141.38	23	0.05	-141.02			
$\mathbf{w}_2$	Ω	1	30020.39	-169.37	1	30079.18	-169.37	1	29676.07	-169.37
	$\Omega+\nu$	2	17889.69	162.63	2	17781.88	162.30	2	18137.11	162.90
	$\Omega-\nu$	3	96.21	38.63	7	96.54	38.96			
	$\Omega+2\nu$	4	3.29	-45.36	37	2.95	-46.02			
	$\Omega-2\nu$	5	0.02	-113.38						

Table 8: Same as table 7 for the system *II* corresponding to the 1999 KW4 binary asteroids.

var.		i	$A_i^{(a)}$ ($''$)	$\varphi_i^{(a)}$ (deg)	i	$A_i^{(f)}$ ($''$)	$\varphi_i^{(f)}$ (deg)	i	$A_i^{(c)}$ ($''$)	$\varphi_i^{(c)}$ (deg)
	Ω	1	27916.13	-152.96	1	27979.55	-153.15	1	27916.04	-152.96
$\mathbf{w}$	$\Omega+\nu$	2	4.65	-152.96	3	4.42	-160.28	2	4.72	-152.96
	$\Omega-\nu$	3	0.02	27.04						
	Ω	1	7991.22	27.04	1	8008.98	26.85	1	7991.22	27.04
$\mathbf{w}_1$	$\Omega+\nu$	2	0.04	27.04	15	0.03	19.72	2	0.04	27.04
	Ω	1	28903.02	-152.96	1	28848.69	-153.15	1	28922.58	-152.96
	$\Omega+\nu$	2	987.12	27.04	2	924.23	18.39	2	1001.81	27.04
$\mathbf{w}_2$	$\Omega-\nu$	3	4.87	-152.96	53	1.48	-146.03			
	$\Omega+2\nu$	4	0.01	27.04						

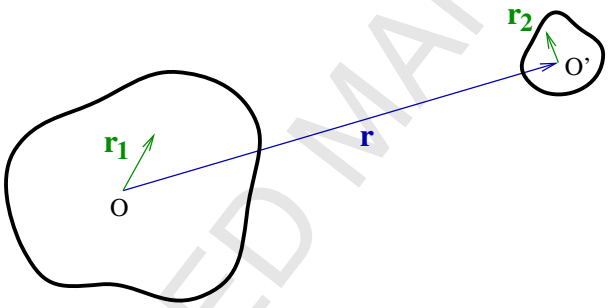

Figure 1: Coordinates definition.

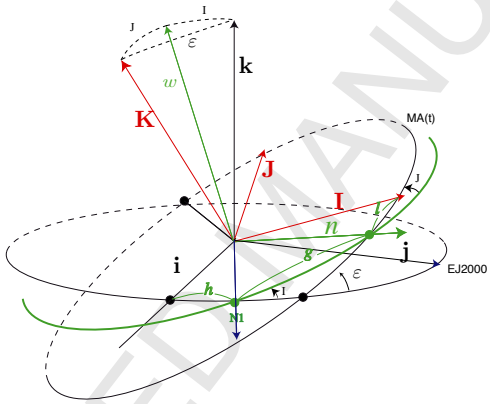

Figure 2: Definition of Andoyer's coordinates. $(\boldsymbol{i}, \boldsymbol{j}, \boldsymbol{k})$ is a fixed reference frame, and $(\boldsymbol{I}, \boldsymbol{J}, \boldsymbol{K})$ the reference frame of the principal axis of inertia of the solid body. The Andoyer action variables are $(G, H = \boldsymbol{G} \cdot \boldsymbol{k}, L = \boldsymbol{G} \cdot \boldsymbol{K})$ with the associated angles (g, h, l) (Andoyer, 1923).

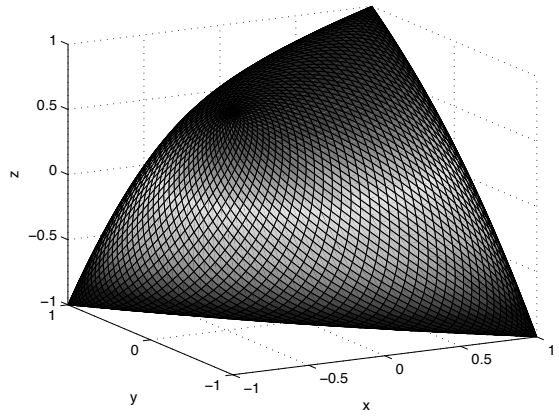

Figure 3: The surface $v^2(x, y, z) = 0$. As $v^2 \geq 0$, the allowed space is the interior of this Cassini berlingot shaped volume.

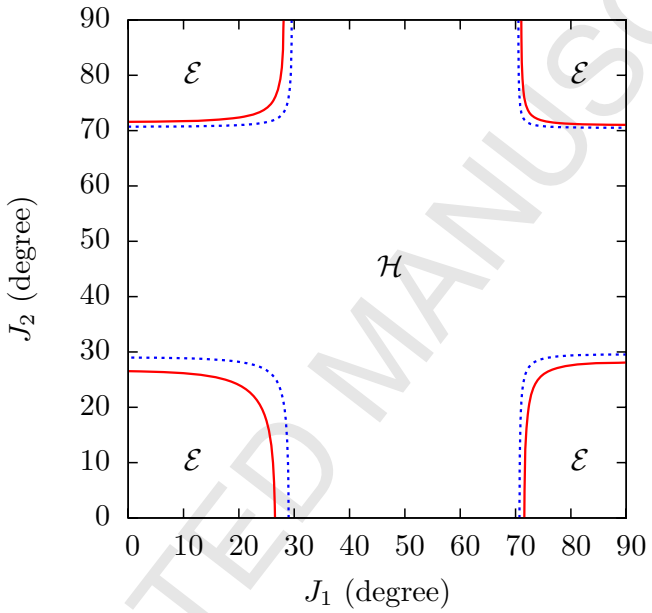

Figure 4: Shape of the surface $\mathcal{Q}'$ as a function of the angles J_1 and J_2 between the angular momentum and the axis of maximum inertia of each bodies. $\mathcal{E}$ and $\mathcal{H}$ stand for ellipsoid and hyperboloid respectively. The solid curve in red delineates the $\mathcal{E}$ and the $\mathcal{H}$ zones for $\eta = 25/9$. The dashed blue curve corresponds to $\eta = 25/4$. See text for details.

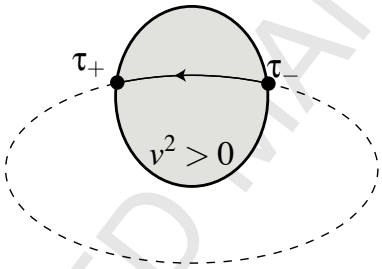

Figure 5: The shaded area corresponds to the region where $v^2 > 0$, inside the Cassini berlingot $\mathcal{B}$. The orbit intersects the Cassini berlingot $\mathcal{B}$ in $t = \tau_+$ and $t = \tau_-$.

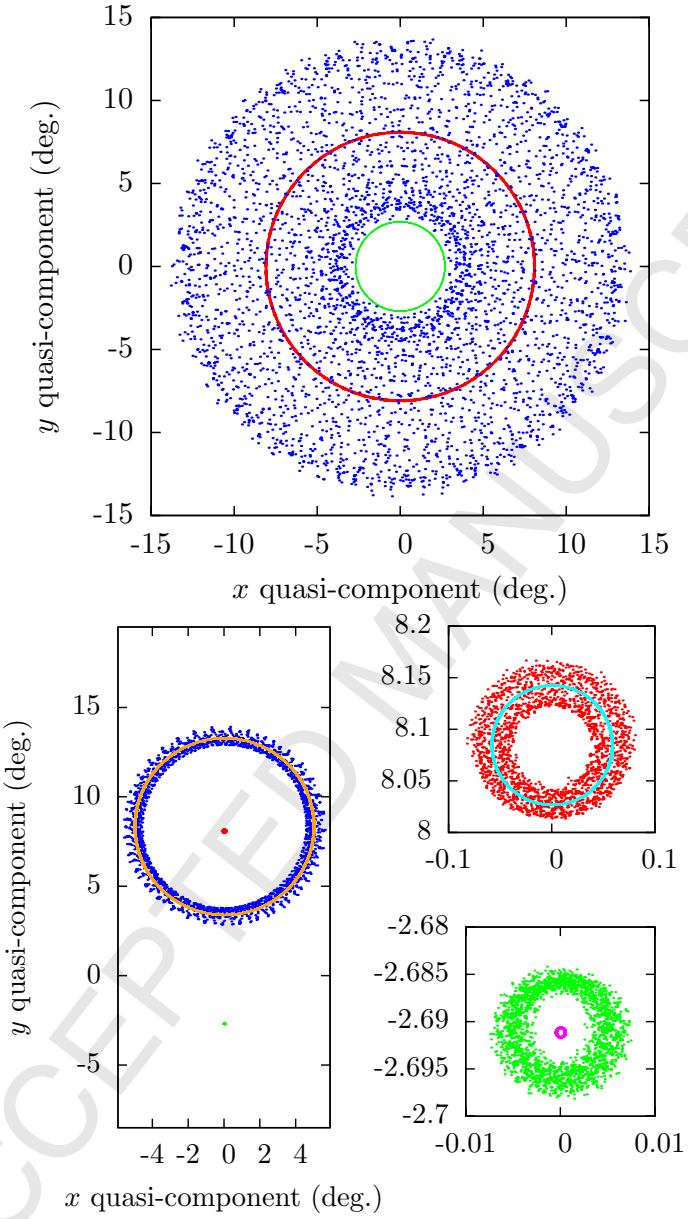

Figure 6: Quasi-projection of the poles $\mathbf{w}$ (red), $\mathbf{w}_1$ (green), $\mathbf{w}_2$ (blue) on the plane perpendicular to the total angular momentum $\boldsymbol{W}_0$, in a fixed reference frame (left panel) and in a frame rotating with the precession period (right panels). The two little figures on the right are zooms on the nutation motion of the orbit (top) and of the primary axis (bottom). The initial conditions and parameters are those of the system I. The vectors $\mathbf{w}$, $\mathbf{w}_1$ and $\mathbf{w}_2$ have been integrated with the full Hamiltonian. In the right panels, the output of the averaged Hamiltonian has been superposed: $\mathbf{w}$ in cyan, $\mathbf{w}_1$ in pink and $\mathbf{w}_2$ in orange.

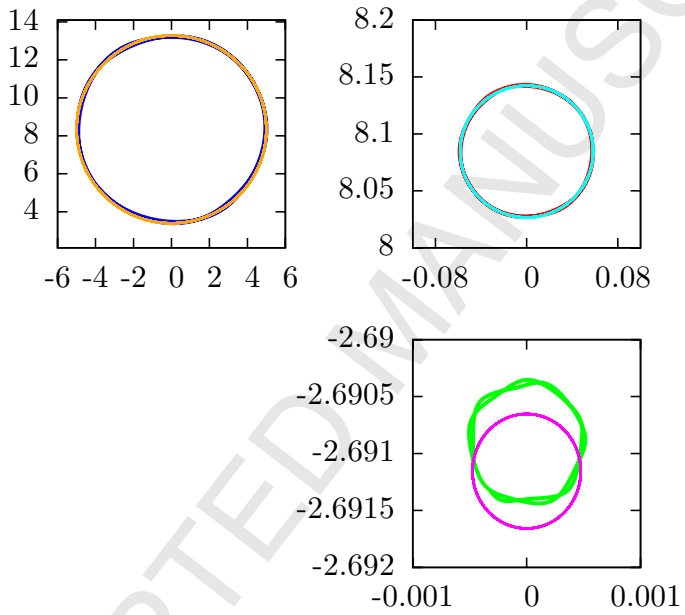

Figure 7: Same as the right panel of Fig. 6. The output of the full Hamiltonian, integrated over 20 days with an output step of 30 min, has been filtered with a low-pass filter with a cutoff frequency equal to 4 rad/day.

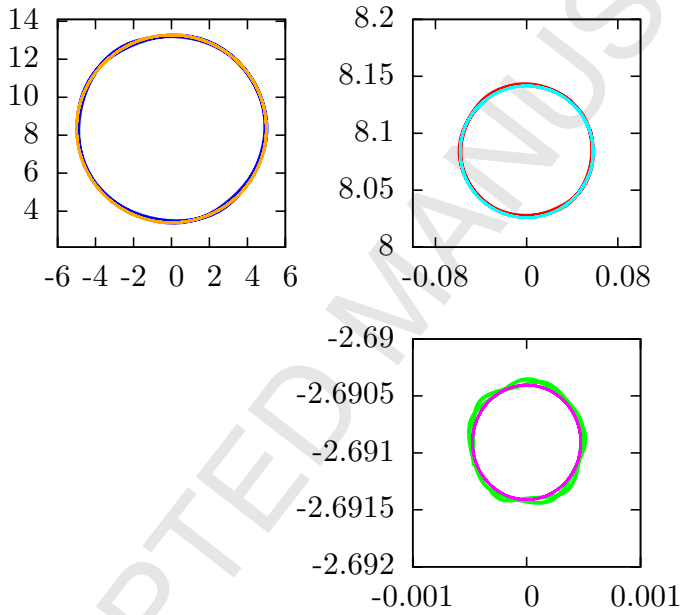

Figure 8: Same as Fig. 7. The initial obliquity of the primary in the averaged Hamiltonian has been decreased by 3.6″.